ISSN 2738-0971
eISSN 2738-1013

Bulletin of Natural Sciences Research

Vol. 12, Nº 1, 2022.

BULLETIN OF NATURAL SCIENCES RESEARCH

Published by
Faculty of Sciences and Mathematics, University of Priština in Kosovska Mitrovica
Republic of Serbia

Focus and Scope

Bulletin of Natural Sciences Research is an international, peer-reviewed, open access journal, published semiannually, both online and in print, by the Faculty of Sciences and Mathematics, University of Priština in Kosovska Mitrovica, Republic of Serbia. The Journal publishes articles on all aspects of research in biology, chemistry, geography, geoscience, astronomy, mathematics, computer science, mechanics and physics.

Editorial Office

Ive Lole Ribara 29; 38220, Kosovska Mitrovica, Serbia, e-mail: editor@bulletinnsr.com, office@bulletinnsr.com; fax: +381 28 425 397

Printed by

Sigraf, Ćrila i Metodija bb, 37000 Kruševac, tel: +38137427704, e-mail: stamparijasigraf@gmail.com

Available Online

This journal is available online. Please visit http://www.bulletinnsr.com to search and download published articles.

BULLETIN OF NATURAL SCIENCES RESEARCH

Vol. 12, N^{o} 1, 2022.

CONTENTS

CHEMISTRY

MATHEMATICS, COMPUTER SCIENCE AND MECHANICS

PHYSICS

Bulletin of Natural Sciences Research
Vol. 12, No. 1, 2022, pp. 1-4.
DOI: https://doi.org/10.5937/bnsr12-28145
Original Scientific Paper

verIDENTIFICATION AND DETERMINATION OF 2,5-DIMETOXY-4-BROMOPHENETHYLAMINE (2C-B) IN REAL SAMPLE BY GC-MS METHODS AND DERIVATIZATION AFTER SPE PREPARATION

VERA LUKIĆ[1], RUŽICA MICIĆ[2], ŽIVANA RADOSAVLJEVIĆ[2*]

[1]Institute of Forensic Medicine, Faculty of Medicine, University of Beograd, Beograd, Serbia
[2]Faculty of Sciences and Mathematics, University of Priština in Kosovska Mitrovica, Kosovska Mitrovica, Serbia

ABSTRACT

The abuse of new psychoactive substances is attracting a lot of attention from the world public. There is an increasing use among young people, who are not aware of the harmful effects of this substances. Some of these substances may have been around for years, but have reemerged in the market in altered chemical forms and launched as legal alternatives to common drugs of abuse. This paper describes application of gas chromatography coupled with mass spectrometry method (GC-MS) to identify 2,5-dimetoxy-4-bromophenethylamine (2C-B) compound in urine sample after solid phase extraxtion and derivatization with N-methyl-bis-trifluoroacetamide (MBTFA). Gas chromatographic separation of TFA derivative of 2C-B (2C-B TFA) was successfully performed using DB-5MS capillary column (5% diphenyl-95% dimethilsiloxane). Selected ion monitoring (SIM) technique was used for qvantitative analyses wich was performed using matrix mached calibratores, whereby good results were achieved. Urine sample wich contained 2C-B was obtained within International Quality Assurance Programme - International Collaborative Exercises (ICE) program organized by the scientific department of United Nations Office on Drugs and Crime (UNODC). The aim of this study was to develop a simple and sensitive method of gas chromatography mass spectrometry (GC-EI-MS) for the identification, extraction and quantitative analysis of 2C-B in the urine sample, which is near the blood remains a priority analyzed matrix in clinical and forensic toxicology.

Keywords: New psychoactive substances (NPS), Phenethylamines, 2-CB, GC-MS method.

INTRODUCTION

New psychoactive substances (NPS, or better known as "legal highs" products) denote synthetically modified natural substances or completely newly designed molecular structures, which lead to a number of harmful effects when consumed, often even ends in death. (National Forensic Service (2014) Special report; Wikström et al., 2013).

This group of compounds includes synthetic cannabinoids, cathinones, phenethylamines, piperazines and tryptamine.

Pheneteliamines are a group of compounds that contain chemical structures that are in fact molecular variants of basic compounds, ie. amphetamines, 3,4-methylenedioxymethamphetamine (MDMA), etc. A series of modifications in the basic structure, which are partially induced by natural products, can significantly change the pharmacological activity, and create a new compound, with completely different effects that occur when consumed. (Jiang et al., 2014; Mahmoud et al., 2014; Choi et al., 2013). 2C-B is a psychedelic drug of the 2C family. It is a group of compounds with a common phenethylamine backbone, which contains two methoxy groups on benzene, at positions 2 and 5, as well as substituents that are different, at position 4 and, very rarely, at position 3. The general structure of 2C compaund and structure of 2C-B are shown in Figure 1 and Figure 2.

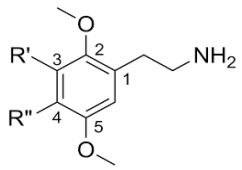

Figure 1. General structure of 2C compound.

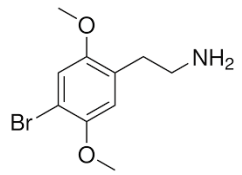

Figure 2. Structure of 2C-B compound.

2C-B (4-bromo-2,5-dimethoxy-b-phenethylamine) formed by benzene substitution, acts as an agonist at 5-HT2 (serotonin 2) receptors. (Cole et al., 2002; Hill et al., 2011).

The GC-MS method can be used to identify and quantify psychoactive compounds, such as cannabinoids, amphetamines, cocaine, antidepressants, antipsychotics, etc. Samples were analyzed by this method after derivatization. (Pujades et al., 2007).

* Corresponding author: zivana.radosavljevic30@gmail.com

This paper presents the application of the GC-MS method for the identification of a newly designed drug, using the SPE for sample preparation and with special emphasis on the derivatization procedure with MBTFA for qualitative and quantitative analysis of the newly designed drug 2C-B in a urine sample. Urine sample was obtained as a part of International Quality Assurance Programme, International Collaborative Exercises program organized by the scientific department of United Nations Office on Drugs and Crime.

EXPERIMENTAL

Materials and methods

Chemical and reagents

All chemicals were purchased in the highest possible purity and used without any further purification. A reference standard of 4-Bromo-2,5-dimetoxyphenethylamine.hydrochloride (2C-B.HCI) with chemical purity declared 99,3 % was purchased from Lipomed AG (Arlesheim, Switzerland). Methanol, ethyl acetate, n-hexane 2-propanol (HPLC grade, 99,9%), ammonium hydroxide (25%), hydrochloric acid (36%) were purchased from Fisher Scientific (Pittsburgh, PA). The derivatization reagent used for the acylation reaction was N-methyl-bis (trifluoroacetamide) (MBTFA), 98%, which was purchased from Macherey–Nagel GmbH & Co. (Düren, Germany). In this study, Strata X-C, 33 µm particle size, Polymeric Strong Cation, 60.0 mg / 3.0 mL, solid-phase extraction (SPE) columns were used and were obtained from Phenomenex (Torrance). Blank urine samples, collected from volunteer laboratory personnel, were used for the development of the method. They were firstly screened by GC/MS to confirm absence of drugs.

Calibration standards

Stock standard solution of 2C-B **were** prepared in methanol at a concentration of 1.0 mg/mL and stored at **−20◦C**. Five working standard solutions containing 2C-B at the following concentrations 5.0, 8.0, 10.0, 12.0, and 15.0 µg/mL, were prepared by mixing the appropriate volumes of the corresponding stock solution and then by diluting with methanol (stroed at -20°C) .

Spiked urine samples for calibration curves (calibrators) were prepared by spiking 1.8 mL of blank human urine with 200.0 µl of working standard solutions. The five calibrators contained 2C-B at concentrations of 0.5, 0.8, 1.0, 1.2 and 1.5 µg/mL.

Sample preparation

Strata-X-C cc (60 mg) columns (Phenomenex) were used for SPE extraction of 2C-B from urine samples (spiked urine samples and urine sample from ICE program). 3 mL of urine sample was acidified with 30.0 µL of 5.0 M HCl. The SPE column was conditionered with 2.0 mL of 0.1 M MeOH and 2.0 mL of deionized water at a rate of 2.0 mL/min. Then 2.0 mL urine sample was loaded at a rate of 2.0 mL/min. Rinsing was made by 2.0 mL of 0.1 M NaOH at a rate of 2 mL/min, 2.0 mL of deionized water at a rate of 8 mL/min and 4.0 mL of hexane at a rate of 8 mL/min. After washing the column, elution was performed with 3.0 mL of 2-propanol/methylene chloride/ammonium hydroxide (80:20:2, v/v/v), at a rate of 2 mL/min. The procedure is followed by acidification and evaporation by adding 100.0 µL of 1% HCl to each tube, before evaporation under N_2. After evaporation of the extract (eluate) samples were derivatized with 50.0 µL of MBTFA (N-methyl-bis-trifluoroacetamide). The reaction was performed at 80°C for 15 min. Reconstitution in 200.0 µL of ethyl acetate is then performed. Gas-chromatographic separation TFA derivative of 2C-B was successfully performed using DB-5MS capillary column (5% diphenyl-95% dimethilsiloxane). External standards method was used for quantification. The calibration curve is constructed using five calibrators, samples of spiked urine in which standard solutions were added to achieve 2-CB concentrations of 0.5, 0.8, 1.0, 1.2 and 1.5 µg/mL respectively (matrix-matched calibrator samples). Urine sample for ICE control program was analyzed after extraction and derivatization in the same way as the spiked samples.

Gas chromatography–mass spectrometry analysis

The GC/MS analysis was performed using a Shimadzu GC-2010 Plus equipped with a Shimadzu AOC-5000 auto sampler system and interfaced with a Shimadzu QP 2010 Ultra mass spectrometer (Shimadzu, Tokyo, Japan).

The GC was equipped with a split /splitless injection port operated at splitless mode. **1.0 µL** of extract injecting into the GC–MS. The separation of analytes was carried out using a cross-linked DB-5MS capillary column (30 m × 0.25 mm i.d.,0.25 um film thickness) supplied by Agilent Technologies (Illinois, IL, USA). Helium was employed as the carrier gas and used at a flow rate of 1.32 mL / min. The temperatures of injection port, ion source and interface were 250, 200 and 280ºC, respectively. Initial oven temperature of 60ºC was held for 2 min, followed by an increase to 280ºC at a rate of 20ºC/min and a final hold time of 4 min, resulting in a total run time of 17 min per sample with a solvent delay of 4.0 min.

Ionization voltage of 70 eV was used to obtained full scan and selected ion monitoring of analytes in the m/z range 50–450 at a scan rate of 3.62 scan/s. The mass spectrometer (MS) was operated in full scan and selected ion monitoring (EI/Scan/SIM and SIM) mode.

RESULTS AND DISCUSSION

Z-score of 0.6 for the our resultat of 1.38 µg/mL of 2C-B in the urine sample, was obtained after evaluation of results by ICE program organizers for round 2013/2 in wich 74 countries was participated.

Figure 3 shows ful scan mass spectrum TFA derivative of 2C-B obtained from urine sample.

For Selected ion monitoring we used tree ions m/z 242, m/z 229 and m/z 148, Figure 4.

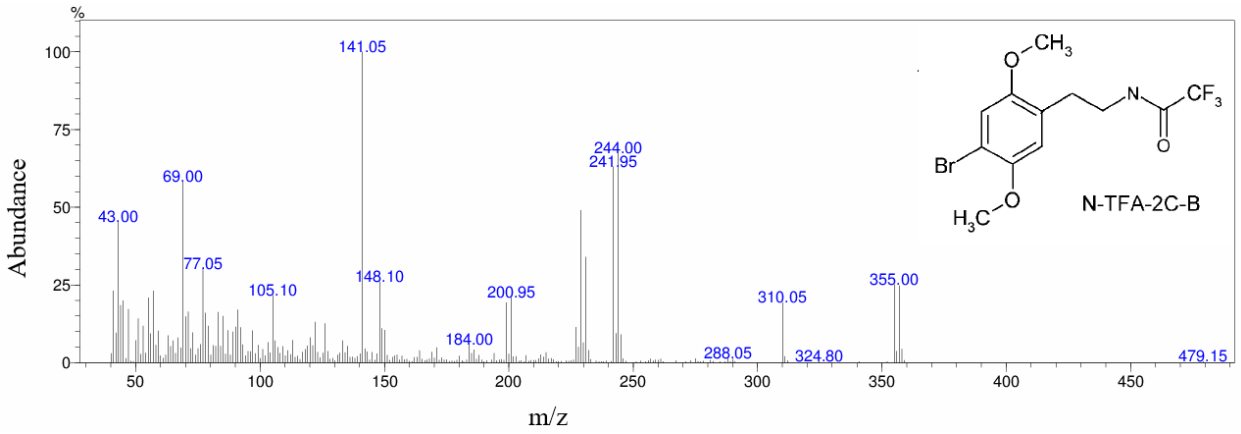

Figure 3. EI GC-MS mass spectrum of TFA derivative of 2C-B.

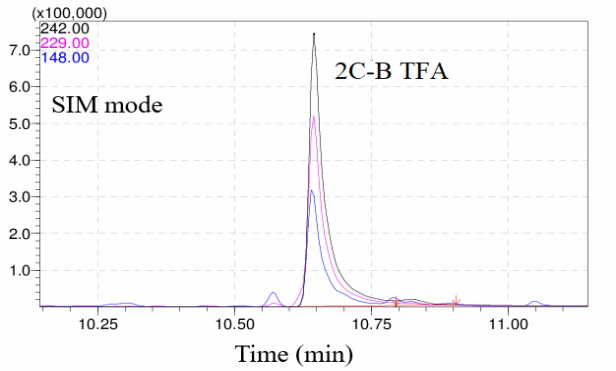

Figure 4. Chromatogram of three ions m/z 242, m/z 229 and m/z 148 using for SIM mode.

Calibration curve, which was constructed using five calibrators, matrix-matched calibrator samples is shown on Figure 5. Obtained correlation coefficient was r 2>0,999. SIM mode was used for quantitative analyses.

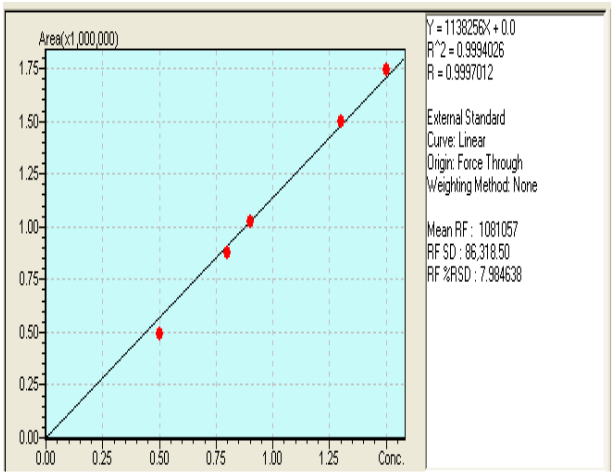

Figure 5. Calibration curve obtained from matrix matched calibrators of 2C-B TFA.

In modern chemical analysis two specific trends can be noticed. One is the requirement for more sensitive and accurate analytical methods and the other for simpler methods that require as little as possible human intervention. Derivatization procedure use specific chemical changes to make analytical methods more sensitive and accurate.

That usualy involve more human intervention than the direct use of advanced instrumentation. For this reason, derivatization is not the first choice when selecting an analytical method. But, the benefits of derivatization in many cases, are more important than the disadvantage of requiring human intervention (Serban, 2018).

The advantages of its use are reflected on changes chemical properties derivatized analytes (higher volatility, better thermal stability) and therefore better separation, selectivity, sensitivity and identification of compounds.

If combined with the GC-MS method, as shown within this study, derivatization can significantly increase the ability to identify new designed drug from phenethylamine group, 2-CB.

Because compound from phenethylamine group (e.g methamphetamine, amphetamine and methylenedioxyphenylalkylamine derivatives, such as 3,4-methylenedioxymethamphetamine (MDMA)) have relatively low molecular weights, high polarity, and volatility, derivatization is necessary when using gas chromatography for analysis biological samples in clinical and forensic toxicology.

There are basically three types of derivatization reactions, such as alkylation (which is the main esterification process), then acylation and silylation. (Orata, 2012).

In this study we were successfully applied acylation as one of the most popular derivatization reactions for primary and secondary amines to 2C-B and obtained stabile 2C-B TFA derivative that gave an enhanced response in GC compared with the parent compound.

CONCLUSIONS

Identification of 2-CB compounds in samples of biological material is very important. With the help of GC-MS method, which is a very reliable and sensitive method, thanks to the library of mass spectra, this is the method of choice, together with derivatization of compounds, a successful analysis was achieved, and the presence of 2-CB compound in urine sample confirmed.

REFERENCES

Choi H., Heo S., Choe S., Yang W., Park Y., Kim E. & Lee J. 2013. Simultaneous analysis of synthetic cannabinoids in the materials seized during drug trafficking using GC-MS. Analytical and bioanalytical chemistry, pp. 3937-3944. doi: 10.1007/s00216-012-6560-z

Cole M. D. & Oxley N. 2002. 4-Bromo-2,5-dimethoxyphenethylamine (2C – B): a review of the public domain literature, Sci. Justice, pp. 223-224. doi: 10.1016/S1355-0306(02)71832-7

Hasegawa C., Kumazawa T., Lee X. P. et al., 2007. Pipette tip solid-phase extraction and gas chromatography-mass spectrometry for the determination of methamphetamine and amphetamine in human whole blood. Analytical and Bioanalytical Chemistry, pp. 563-570. doi: 10.1007/s00216-007-1460-3

Hill S. L. & Thomas S. H. 2011. Clinical toxicology of newer recreational drugs. Clin. Toxicol. (Phila.), pp. 705-719. doi: 10.3109/15563650.2011.615318.

Jiang YB., Zhong M. & Ma YY. 2014. The rapid selecting of precursor ions and product ions of thirty-four kinds of pesticide for content determination by GC-EI/MS/MS Food control, pp. 110-114. doi.org/10.1016/j.foodcont.2014.03.004

Mahmoud A. EISohly, Gul W., S. Wanas A. & Mohamed M. Radwan 2014. Synthetic cannabinoids: Analysis and metabolites, Life Sciences, pp.78-90. doi: 10.1016/j.lfs.2013.12.212.

Mass spectral libraries were downloaded from Scientific Working Group for the Analysis of Seized Drugs (SWGDRUG) website http://www.swgdrug.org

National Forensic Service (2014) Special report. The type of new psychoactive substances abused in Korea: case report and recent trend. National Forensic Service, Seoul, pp 6-7. doi.org/10.1007/s11419-015-0286-5

Orata F. 2012. Derivatization reactions and reagents for gas chromatography analysis. In book: Advanced Gas Chromatography - Progress in Agricultural, Biomedical and Industrial Applications, DOI: 10.5772/33098

Pujadas M., Pichini S., Civit E., Santamarina E., Perez K. & de la Torre R. 2007. A simple and reliable procedure for the determination of psychoactive drugs in oral fluid by gas chromatography – mass spectrometry, J. Pharm. Biomed. Anal., pp. 594-601. doi.org/10.1016/j.talanta.2021.122966

Pujadas M., Pichini S., Poudevida S. et al., 2003. Development and validation of a gas chromatography-mass spectrometry assay for hair analysis of amphetamine, methamphetamine and methylenedioxy derivatives. Journal of Chromatography B, pp. 249-255. doi: 10.1016/j.jchromb.2003.09.056

Recommended methods for the Identification and Analysis of Synthetic Cannabinoid Receptor Agonists in Seized Materials - United nations office on drugs and crime, May 2013 (http://www.unodc.org/)

Serban C. M. & Victor D. 2018. Derivatization Methods in GC and GC/MS, In book: Gas Chromatography - Derivatization, Sample Preparation, Application DOI: 10.5772/INTECHOPEN.81954

Villamor J. L., Bermejo A. M., Fernández P. & Tabernero M. J. 2005. A new GC-MS method for the determination of five amphetamines in human hair. Journal of Analytical Toxicology, pp. 135-139. doi.org/10.1093/jat/29.2.135

Villamor J. L., Bermejo A. M., Fernandez P., Weinmann W, Renz M, Vogt S. & Pollak S. 2000. Automated solid-phase extraction and two-step derivatisation for simultaneous analysis of basic illicit drugs in serum by GC/MS. International Journal of Legal Medicine, pp. 229-235. DOI: 10.1007/s004149900098

Wikström M., Dahlgren M. & Kronstrand R. 2013. An accidental fatal intoxication with methoxetamine. J. Anal. Toxicol., pp. 43-46. DOI: 10.1093/jat/bks086

Bulletin of Natural Sciences Research
Vol.12, No.1, 2022, pp. 5-10.

DOI: https://doi.org/10.5937/bnsr12-34903
Original Scientific Paper

GENERALIZED α-MIN SPECIAL TYPE CONTRACTION RESULTS ON 2-MENGER SPACES

SAMIR KUMAR BHANDARI[1,⋆], **SUMIT CHANDOK**[2]

[1]Department of Mathematics, Bajkul Milani Mahavidyalaya, P.O- Kismat Bajkul, Dist - Purba Medinipur, Bajkul, West Bengal - 721655, India.
[2]School of Mathematics, Thapar Institute of Engineering and Technology, Patiala-147004, Punjab, India.

ABSTRACT

The goal of this paper is to present some novel probabilistic α-minimum contraction results on probabilistic 2-metric spaces. Our findings are based on probabilistic 2-metric spaces, which are the probabilistic generalisations of 2-metric spaces. An illustrative example backs up our findings.

Keywords: 2-Menger spaces, Cauchy sequence, Fixed point, ϕ-function, Altering distance function.

INTRODUCTION

Fixed point theory and its applications are important areas of study in mathematics. Metric fixed point theory is used in differential calculus, integral calculus, optimization problems, matrix equations, and a variety of other disciplines of study. Probabilistic 2-metric spaces (2-PMS), which are the probabilistic generalisation of 2-metric spaces, are studied in this paper. Zeng (1987) pioneered these spaces in which distribution function plays the role of metric. 2-Menger spaces are probabilistic 2-metric spaces in which the triangle inequality is hypothesised using the t-norm. Khan et al. (1984) developed the innovative notion of altering distance function in 1984. The "altering distance function" is a control function that changes the distance between two points in metric space. In Choudhury & Das (2008), the concept of changing the distance function has recently been expanded to the context of Menger spaces. This control function is referred to as the ϕ-function, and it is extremely useful for proving fixed point conclusions in Menger spaces. This approach is also applicable to many other situations in this area, such as coincidence point problems. Some recent works using ϕ-function are mentioned in Bhandari (2017a); Bhandari & Choudhury (2017); Bhandari (2017b); Choudhury et al. (2012); Dutta et al. (2009). In recent research works, probabilistic metric (PM) spaces have an important role. Many authors have established various types of results on this popular directions. Some generalized works in this line may be referred as Kutbi et al. (2015); Mihet (2009).

Main features of this paper are following:
1. A new probabilistic α − min special type contraction result.
2. For such contraction, unique fixed point is obtained.
3. Here we use a control function.
4. An illustrative example validates our theorem.

PRELIMINARIES

Some important definitions and mathematical preliminaries are discussed in this section. These are helpful to prove our main results.

Definition 1. A distribution function (see Hadzic & Pap (2001); Schweizer & Sklar (1983)) is a mapping $\Gamma : \mathbb{R} \to \mathbb{R}^+$ if it is non-decreasing and left continuous with $\inf_{\eta\in\mathbb{R}} \Gamma(\eta) = 0$ and $\sup_{\eta\in\mathbb{R}} \Gamma(\eta) = 1$, where $\mathbb{R}$ is the set of reals and $\mathbb{R}^+$ is the set of non-negative reals respectively.

This function has an very important role in our present discussion.

Definition 2. A probabilistic metric space (briefly, PM-space) Hadzic & Pap (2001); Schweizer & Sklar (1983) is an ordered pair (S, Γ), where S is a non-empty set and Γ is a mapping from $S \times S$ into the set of all distribution functions. The function $\Gamma_{\kappa,\mu}$ is assumed to satisfy the following conditions for all $\kappa, \mu, \nu \in S$,

(i) $\Gamma_{\kappa,\mu}(0) = 0$,
(ii) $\Gamma_{\kappa,\mu}(\eta) = 1$ for all $\eta > 0$ if and only if $\kappa = \mu$,
(iii) $\Gamma_{\kappa,\mu}(\eta) = \Gamma_{\mu,\kappa}(\eta)$ for all $\eta > 0$,
(iv) if $\Gamma_{\kappa,\mu}(\eta_1) = 1$ and $\Gamma_{\mu,\nu}(\eta_2) = 1$ then $\Gamma_{\kappa,\nu}(\eta_1 + \eta_2) = 1$ for all $\eta_1, \eta_2 > 0$.

The theory on these spaces have been discussed vastly in the book of Schweizer and Sklar Schweizer & Sklar (1983).

Example 3. Let $S = [0, 7]$ and $\Gamma_{\kappa,\mu}(\eta) = \frac{\eta}{\eta+|\kappa-\mu|}$, then (S, Γ) is a PM space.

Shi et al. (2003) introduced the following definition of n-th order t-norm. It is a function which is used to construct our main results.

Definition 4. A mapping $T : \Pi_{i=1}^{n}[0, 1] \to [0, 1]$ is called a n-th order t-norm if the following conditions are satisfied:

⋆ Corresponding author: skbhit@gmail.com

(i) $T(0,0,\ldots,0)=0$, $T(a,1,1,\ldots,1)=a$ for all $a\in[0,1]$,
(ii) $T(a_1,a_2,,a_3,\ldots,a_n) = T(a_2,a_1,a_3,\ldots,a_n) = T(a_2,a_3,a_1,\ldots,a_n) = \ldots = T(a_2,a_3,a_4,\ldots,a_n,a_1)$,
(iii) $a_i \geq b_i$, $i=1,2,3,\ldots,n$, implies $T(a_1,a_2,a_3,\ldots,a_n) \geq T(b_1,b_2,b_3,\ldots,b_n)$,
(iv) $T(T(a_1,a_2,a_3,\ldots,a_n),b_2,b_3,\ldots,b_n)$
$= T(a_1,T(a_2,a_3,\ldots,a_n,b_2),b_3,\ldots,b_n)$
$= T(a_1,a_2,T(a_3,a_4,\ldots,a_n,b_2,b_3),b_4,\ldots,b_n)$
$\vdots$
$= T(a_1,a_2,\ldots,a_{n-1},T(a_n,b_2,b_3,\ldots,b_n))$.

When $n=2$, we have a binary t-norm, which is commonly known as t-norm.

In this paper we use third order minimum t-norm. The following are the examples of different types of third order t-norms:

(i) The minimum t-norm, $\Delta = T_m$, defined by $T_m(a,b,c) = \min\{a,b,c\}$.
(ii) The product t-norm, $\Delta = T_p$, defined by $T_p(a,b,c) = a.b.c$.
(iii) The Lukasiewicz t-norm, $\Delta = T_L$, defined by $T_L(a,b,c) = \max\{a+b+c-1,0\}$.

Menger spaces (see Hadzic & Pap (2001); Schweizer & Sklar (1983)) are the particular types of probabilistic metric spaces. The definition is given below.

Definition 5. A Menger space is a triplet (S,Γ,Δ), where S is a non empty set, Γ is a function defined on $S\times S$ to the set of all distribution functions and Δ is a t-norm, such that the following are satisfied:

(i) $\Gamma_{\kappa,\mu}(0)=0$ for all $\kappa,\mu\in S$,
(ii) $\Gamma_{\kappa,\mu}(s)=1$ for all $s>0$ if and only if $\kappa=\mu$,
(iii) $\Gamma_{\kappa,\mu}(s)=\Gamma_{\mu,\kappa}(s)$ for all $\kappa,\mu\in S$, $s>0$ and
(iv) $\Gamma_{\kappa,\mu}(u+v)\geq \Delta(\Gamma_{\kappa,\nu}(u),\Gamma_{\nu,\mu}(v))$ for all $u,v\geq 0$ and $\kappa,\mu,\nu\in S$.

A metric space becomes a Menger probabilistic metric space if we write $\Gamma_{\kappa,\mu}(\eta) = H(\eta - d(\kappa,\mu))$ where H is the Heavyside function given by

$$H(\eta)=\begin{cases}1 \text{ if } & \eta>0,\\ 0 \text{ if } & \eta\leq 0.\end{cases}$$

In 1963, S. Gähler (see Gähler (1963, 1965)) introduced the concept of 2-metric spaces. In metric spaces we consider a real valued function d on $S\times S$ but here we consider the real valued function d on $S\times S\times S$.

Definition 6. Let S be a non empty set. A real valued function d on $S\times S\times S$ is said to be a 2-metric on S if for all $\kappa,\mu,\nu,w\in S$,

(i) given distinct elements $\kappa,\mu\in S$, there exists an element ν of S such that
$$d(\kappa,\mu,\nu)\neq 0,$$
(ii) $d(\kappa,\mu,\nu)=0$ when at least two of κ,μ,ν are equal,
(iii) $d(\kappa,\mu,\nu)=d(\kappa,\nu,\mu)=d(\mu,\nu,\kappa)$,
(iv) $d(\kappa,\mu,\nu)\leq d(\kappa,\mu,w)+d(\kappa,w,\nu)+d(w,\mu,\nu)$.

When d is a 2-metric on S, the ordered pair (S,d) is called a 2-metric space.

Example 7. If we consider three vertices κ,μ,ν of a triangle, then area of triangle may be taken as $d(\kappa,\mu,\nu)$. Then the metric function d satisfies all the conditions of 2-metric.

A probabilistic 2-metric space is a probabilistic generalization of 2-metric space. In 1987, Zeng Zeng (1987) introduced the concept of probabilistic 2-metric spaces.

Definition 8. A probabilistic 2-metric space is an order pair (S,Γ) where S is an arbitrary set and Γ is a mapping from $S\times S\times S$ into the set of all distribution functions such that the following conditions are satisfied:

(i) $\Gamma_{\kappa,\mu,\nu}(\eta)=0$ for $\eta\leq 0$ and for all $\kappa,\mu,\nu\in S$,
(ii) $\Gamma_{\kappa,\mu,\nu}(\eta)=1$ for all $\eta>0$ if and only if at least two of κ,μ,ν are equal,
(iii) for distinct points $\kappa,\mu\in S$, there exists a point $\nu\in S$ such that $\Gamma_{\kappa,\mu,\nu}(\eta)\neq 1$ for $\eta>0$,
(iv) $\Gamma_{\kappa,\mu,\nu}(\eta)=\Gamma_{\kappa,\nu,\mu}(\eta)=\Gamma_{\nu,\mu,\kappa}(\eta)$ for all $\kappa,\mu,\nu\in S$ and $\eta>0$,
(v) $\Gamma_{\kappa,\mu,w}(\eta_1)=1$, $\Gamma_{\kappa,w,\nu}(\eta_2)=1$ and $\Gamma_{w,\mu,\nu}(\eta_3)=1$ then $\Gamma_{\kappa,\mu,\nu}(\eta_1+\eta_2+\eta_3)=1$, for all $\kappa,\mu,\nu,w\in S$ and $\eta_1,\eta_2,\eta_3>0$.

Example 9. Let $\Gamma_{\kappa,\mu,\nu}(\eta)=\begin{cases}\frac{\eta}{\eta+\min|\kappa-\mu|,|\kappa-\nu|,|\mu-\nu|} & \text{if } \eta>0,\\ 0, & \text{if } \eta\leq 0,\end{cases}$
for all $(\kappa,\mu,\nu)\in S^3$. Then (S,Γ) is a probabilistic 2-metric spaces.

In Menger spaces, we use a function Γ which is defined on $S\times S$ to the set of all distribution functions but in case of 2-Menger spaces (see Shih-sen & Nan-Jing (1989)) we use the function Γ which is defined on $S\times S\times S$ to the set of all distribution functions.

Definition 10. Let S be a nonempty set. A triplet (S,Γ,Δ) is said to be a 2-Menger space if Γ is a mapping from $S\times S\times S$ into the set of all distribution functions satisfying the following conditions:

(i) $\Gamma_{\kappa,\mu,\nu}(0)=0$,
(ii) $\Gamma_{\kappa,\mu,\nu}(\eta)=1$ for all $\eta>0$ if and only if at least two of $\kappa,\mu,\nu\in S$ are equal,
(iii) for distinct points $\kappa,\mu\in S$ there exists a point $\nu\in S$ such that $\Gamma_{\kappa,\mu,\nu}(\eta)\neq 1$ for $\eta>0$,
(iv) $\Gamma_{\kappa,\mu,\nu}(\eta)=\Gamma_{\kappa,\nu,\mu}(\eta)=\Gamma_{\nu,\mu,\kappa}(\eta)$, for all $\kappa,\mu,\nu\in S$ and $\eta>0$,
(v) $\Gamma_{\kappa,\mu,\nu}(\eta)\geq\Delta(\Gamma_{\kappa,\mu,w}(\eta_1),\Gamma_{\kappa,w,\nu}(\eta_2),\Gamma_{w,\mu,\nu}(\eta_3))$

where $\eta_1,\eta_2,\eta_3>0$, $\eta_1+\eta_2+\eta_3=\eta$, $\kappa,\mu,\nu,w\in S$ and Δ is the 3rd order t norm.

Definition 11. Hadzic (1994) A sequence $\{\kappa_n\}$ in a 2-Menger space (S,Γ,Δ) is said to be converge to a limit κ if given $\epsilon>0, 0<\lambda<1$ there exists a positive integer $N_{\epsilon,\lambda}$ such that
$$\Gamma_{\kappa_n,\kappa,a}(\epsilon)\geq 1-\lambda \tag{1.1}$$
for all $n>N_{\epsilon,\lambda}$ and for every $a\in S$.

Definition 12. Hadzic (1994) A sequence $\{\kappa_n\}$ in a 2-Menger space (S, Γ, Δ) is said to be a Cauchy sequence in S if given $\epsilon > 0, 0 < \lambda < 1$ there exists a positive integer $N_{\epsilon,\lambda}$ such that

$$\Gamma_{\kappa_n,\kappa_m,a}(\epsilon) \geq 1 - \lambda \tag{1.2}$$

for all $m, n > N_{\epsilon,\lambda}$ and for every $a \in S$.

In our main theorem we have used a complete 2-Menger spaces. Completeness property of spaces have an important role in our results.

Definition 13. Hadzic (1994) A 2-Menger space (S, Γ, Δ) is said to be complete if every Cauchy sequence is convergent in S.

We use the following control function Φ which Choudhury et al. presented in Choudhury & Das (2008).

Definition 14. A function $\phi : R \to R^+$ is said to be a Φ-function if it satisfies the following conditions:

(i) $\phi(\eta) = 0$ if and only if $\eta = 0$,
(ii) $\phi(\eta)$ is strictly monotone increasing and $\phi(\eta) \to \infty$ as $\eta \to \infty$,
(iii) ϕ is left continuous in $(0, \infty)$,
(iv) ϕ is continuous at 0.

Example 15. $\phi(\eta) = \eta^2$, $\phi(\eta) = \sqrt{\eta}$, $\phi(\eta) = \eta$ are some examples of Φ-function.

In numerous research works, many authors Choudhury & Bhandari (2014); Choudhury et al. (2015); Choudhury & Bhandari (2016) use this exciting property.

MAIN RESULTS

Motivated by Dutta et al. (2009); Gopal et al. (2014), we begin this section by introducing the concept of $\alpha -$ min special type contraction and α-admissible mappings in 2-Menger spaces.

Definition 16. Let (S, Γ, Δ) be a 2-Menger space and $h : S \to S$ be a mapping. We say that h is an $\alpha -$ min special type contraction mapping if there exits function $\alpha : S \times S \times (0, \infty) \to \mathbb{R}^+$ satisfying the following inequality

$$\begin{aligned}&\alpha(\kappa, \mu, \eta)\left(\frac{1}{\Gamma_{h\kappa,h\mu,a}(\phi(\eta))} - 1\right)\\ &\leq \min\left(\frac{1}{\Gamma_{\kappa,\mu,a}(\phi(\frac{\eta}{c}))} - 1, \frac{1}{\Gamma_{\kappa,h\kappa,a}(\phi(\frac{\eta}{c}))} - 1, \frac{1}{\Gamma_{\mu,h\mu,a}(\phi(\frac{\eta}{c}))} - 1\right)\end{aligned} \tag{1}$$

for all $\kappa, \mu, a \in S$, $\eta > 0$, where $0 < c < 1$, $\phi \in \Phi$.

Definition 17. Let (S, Γ, Δ) be a 2- Menger space, $h : S \to S$ be a given mapping and $\alpha : S \times S \times (0, \infty) \to \mathbb{R}^+$ be a function, we say that h is α-admissible if for all $\kappa, \mu, a \in S$, and $\eta > 0$, we have

$$\alpha(\kappa, \mu, \eta) \geq 1 \Rightarrow \alpha(h\kappa, h\mu, \eta) \geq 1.$$

Theorem 18. *Let (S, Γ, Δ) be a complete 2-Menger space, Δ is a minimum t-norm and $h : S \to S$ be an $\alpha -$ min special type contraction mapping satisfying the following conditions:*

(i) h is α-admissible,
(ii) there exists $\kappa_0 \in S$ such that $\alpha(\kappa_0, h\kappa_0, \eta) \geq 1$, for all $\eta > 0$,
(iii) if $\{\kappa_n\}$ is a sequence in S such that $\alpha(\kappa_n, \kappa_{n+1}, \eta) \geq 1$ for all $n \in \mathbb{N}$ and for all $\eta > 0$.

Then h has a unique fixed point, that is, there exists a point $\kappa \in S$ such that $h\kappa = \kappa$.

Proof. Let $\kappa_0 \in S$ be such that $\alpha(\kappa_0, h\kappa_0, \eta) \geq 1$ for all $\eta > 0$. We consider a sequence $\{\kappa_n\}$ in S so that $\kappa_{n+1} = h\kappa_n$, for all $n \in \mathbb{N}$, where $\mathbb{N}$ is the set of natural numbers. Clearly, $\kappa_{n+1} \neq \kappa_n$ for all $n \in N$, otherwise h has trivially a fixed point.
As h is α-admissible, we get $\alpha(\kappa_0, h\kappa_0, \eta) = \alpha(\kappa_0, \kappa_1, \eta) \geq 1$ implies $\alpha(h\kappa_0, h\kappa_1, \eta) = \alpha(\kappa_1, \kappa_2, \eta) \geq 1$. Also, by induction, we get

$$\alpha(\kappa_n, \kappa_{n+1}, \eta) \geq 1, \text{ for all } n \in \mathbb{N} \text{ and for all } \eta > 0.$$

From the properties of function ϕ, we can find $\eta > 0$ such that $\Gamma_{\kappa_0,\kappa_1,a}(\phi(\eta)) > 0$, for all $a \in S$.

Now, using (1) for all $a \in S$, $\eta > 0$ and $c \in (0, 1)$, we get

$$\begin{aligned}\frac{1}{\Gamma_{\kappa_{n+1},\kappa_n,a}(\phi(\eta))} - 1 &= \frac{1}{\Gamma_{h\kappa_n,h\kappa_{n-1},a}(\phi(\eta))} - 1\\ &\leq \alpha(\kappa_n, \kappa_{n-1}, \eta)\frac{1}{\Gamma_{h\kappa_n,h\kappa_{n-1},a}(\phi(\eta))} - 1\\ &\leq \min\left(\frac{1}{\Gamma_{\kappa_n,\kappa_{n-1},a}(\phi(\frac{\eta}{c}))} - 1, \frac{1}{\Gamma_{\kappa_n,h\kappa_n,a}(\phi(\frac{\eta}{c}))} - 1,\right.\\ &\quad \left.\frac{1}{\Gamma_{\kappa_{n-1},h\kappa_{n-1},a}(\phi(\frac{\eta}{c}))} - 1\right)\\ &= \min\left(\frac{1}{\Gamma_{\kappa_n,\kappa_{n-1},a}(\phi(\frac{\eta}{c}))} - 1, \frac{1}{\Gamma_{\kappa_n,\kappa_{n+1},a}(\phi(\frac{\eta}{c}))} - 1,\right.\\ &\quad \left.\frac{1}{\Gamma_{\kappa_{n-1},\kappa_n,a}(\phi(\frac{\eta}{c}))} - 1\right)\\ &= \min\left(\frac{1}{\Gamma_{\kappa_{n+1},\kappa_n,a}(\phi(\frac{\eta}{c}))} - 1, \frac{1}{\Gamma_{\kappa_n,\kappa_{n-1},a}(\phi(\frac{\eta}{c}))} - 1\right).\end{aligned} \tag{2}$$

The above inequality holds since $\alpha(\kappa_n, \kappa_{n-1}, \eta) \geq 1$.

We now claim that for all $a \in S$, $\eta > 0$, $n \geq 1$ and $c \in (0, 1)$,

$$\min\left(\frac{1}{\Gamma_{\kappa_{n+1},\kappa_n,a}(\phi(\frac{\eta}{c}))} - 1, \frac{1}{\Gamma_{\kappa_n,\kappa_{n-1},a}(\phi(\frac{\eta}{c}))} - 1\right) = \frac{1}{\Gamma_{\kappa_n,\kappa_{n-1},a}(\phi(\frac{\eta}{c}))} - 1, \tag{3}$$

holds.

If possible, let for some $s > 0$,

$$\min\left(\frac{1}{\Gamma_{\kappa_{n+1},\kappa_n,a}(\phi(\frac{s}{c}))} - 1, \frac{1}{\Gamma_{\kappa_n,\kappa_{n-1},a}(\phi(\frac{s}{c}))} - 1\right) = \frac{1}{\Gamma_{\kappa_{n+1},\kappa_n,a}(\phi(\frac{s}{c}))} - 1,$$

then using (2), we get

$$\frac{1}{\Gamma_{\kappa_{n+1},\kappa_n,a}(\phi(s))} - 1 \leq \frac{1}{\Gamma_{\kappa_{n+1},\kappa_n,a}(\phi(\frac{s}{c}))} - 1,$$

that is,

$$\Gamma_{\kappa_{n+1},\kappa_n,a}(\phi(s)) \geq \Gamma_{\kappa_{n+1},\kappa_n,a}(\phi(\frac{s}{c})), \tag{4}$$

which is impossible for all $c \in (0,1)$ (For $\phi(\eta)$ is strictly monotone increasing, $\phi(\frac{s}{c}) > \phi(s)$, that is, $\Gamma_{\kappa_{n+1},\kappa_n,a}(\phi(\frac{s}{c})) \geq \Gamma_{\kappa_{n+1},\kappa_n,a}(\phi(s))$, by the monotone property of Γ). Then, for all $\eta > 0$ and $a \in S$, we get

$$\frac{1}{\Gamma_{\kappa_{n+1},\kappa_n,a}(\phi(\eta))} - 1 \leq \frac{1}{\Gamma_{\kappa_n,\kappa_{n-1},a}(\phi(\frac{\eta}{c}))} - 1,$$

that is,

$$\begin{aligned}
\Gamma_{\kappa_{n+1},\kappa_n,a}(\phi(\eta)) &\geq \Gamma_{\kappa_n,\kappa_{n-1},a}(\phi(\frac{\eta}{c})) \\
&\geq \Gamma_{\kappa_{n-1},\kappa_{n-2},a}(\phi(\frac{\eta}{c^2})) \\
&\vdots \\
&\geq \Gamma_{\kappa_1,\kappa_0,a}(\phi(\frac{\eta}{c^n})).
\end{aligned}$$

Hence

$$\Gamma_{\kappa_{n+1},\kappa_n,a}(\phi(\eta)) \geq \Gamma_{\kappa_1,\kappa_0,a}(\phi(\frac{\eta}{c^n})). \tag{5}$$

Now, taking limit $n \to \infty$ on both sides of (5), for all $\eta > 0$ and $a \in S$, we obtain

$$\lim_{n\to\infty} \Gamma_{\kappa_{n+1},\kappa_n,a}(\phi(\eta)) = 1. \tag{6}$$

Now, we have to prove that $\{\kappa_n\}$ is a Cauchy sequence. On the contrary, there exist $\epsilon > 0$ and $0 < \lambda < 1$ for which we can find subsequences $\{\kappa_{m(\ell)}\}$ and $\{\kappa_{n(\ell)}\}$ of $\{\kappa_n\}$ with $m(\ell) > n(\ell) > \ell$ such that

$$\Gamma_{\kappa_{m(\ell)},\kappa_{n(\ell)},a}(\epsilon) < 1 - \lambda. \tag{7}$$

We take $m(\ell)$ corresponding to $n(\ell)$ to be the smallest integer satisfying (7), so that

$$\Gamma_{\kappa_{m(\ell)-1},\kappa_{n(\ell)},a}(\epsilon) \geq 1 - \lambda. \tag{8}$$

If $\epsilon_1 < \epsilon$ then we have

$$\Gamma_{\kappa_{m(\ell)},\kappa_{n(\ell)},a}(\epsilon_1) \leq \Gamma_{\kappa_{m(\ell)},\kappa_{n(\ell)},a}(\epsilon).$$

So, it is feasible to construct $\{\kappa_{m(\ell)}\}$ and $\{\kappa_{n(\ell)}\}$ with $m(\ell) > n(\ell) > \ell$ and satisfying (7), (8) whenever ϵ is replaced by a smaller positive value. By the continuity of ϕ at 0 and strictly monotone increasing property with $\phi(0) = 0$, it is possible to find $\epsilon_2 > 0$ such that $\phi(\epsilon_2) < \epsilon$.

Then, by the above condition, it is possible to get an increasing sequence of integers $\{m(\ell)\}$ and $\{n(\ell)\}$ with $m(\ell) > n(\ell) > \ell$ such that

$$\Gamma_{\kappa_{m(\ell)},\kappa_{n(\ell)},a}(\phi(\epsilon_2)) < 1 - \lambda, \tag{9}$$

and

$$\Gamma_{\kappa_{m(\ell)-1},\kappa_{n(\ell)},a}(\phi(\epsilon_2)) \geq 1 - \lambda. \tag{10}$$

Now, from (9), we get

$$1 - \lambda > \Gamma_{\kappa_{m(\ell)},\kappa_{n(\ell)},a}(\phi(\epsilon_2)),$$

that is,

$$\frac{1}{1-\lambda} < \frac{1}{\Gamma_{\kappa_{m(\ell)},\kappa_{n(\ell)},a}(\phi(\epsilon_2))},$$

that is,

$$\frac{1}{1-\lambda} - 1 < \frac{1}{\Gamma_{\kappa_{m(\ell)},\kappa_{n(\ell)},a}(\phi(\epsilon_2))} - 1.$$

using the inequality (1), we get

$$\begin{aligned}
\frac{\lambda}{1-\lambda} &< \frac{1}{\Gamma_{\kappa_{m(\ell)},\kappa_{n(\ell)},a}(\phi(\epsilon_2))} - 1 \\
&\leq \alpha(\kappa_{m(\ell)-1}, \kappa_{n(\ell)-1}, \eta)(\frac{1}{\Gamma_{h\kappa_{m(\ell)-1},h\kappa_{n(\ell)-1},a}(\phi(\epsilon_2))} - 1) \\
&\leq \min(\frac{1}{\Gamma_{\kappa_{m(\ell)-1},\kappa_{n(\ell)-1},a}(\phi(\frac{\epsilon_2}{c}))} - 1, \frac{1}{\Gamma_{\kappa_{m(\ell)-1},\kappa_{m(\ell)},a}(\phi(\frac{\epsilon_2}{c}))} - 1, \\
&\quad \frac{1}{\Gamma_{\kappa_{n(\ell)-1},\kappa_{n(\ell)},a}(\phi(\frac{\epsilon_2}{c}))} - 1).
\end{aligned} \tag{11}$$

Now, we can choose $\beta_1, \beta_2 > 0$ such that

$$\begin{aligned}
&\Gamma_{\kappa_{m(\ell)-1},\kappa_{n(\ell)-1},a}(\phi(\frac{\epsilon_2}{c})) \\
&\geq \Delta(\Gamma_{\kappa_{m(\ell)-1},\kappa_{n(\ell)-1},\kappa_{n(\ell)}}(\beta_1), \Gamma_{\kappa_{m(\ell)-1},\kappa_{n(\ell)},a}(\phi(\epsilon_2)), \Gamma_{\kappa_{n(\ell)},\kappa_{n(\ell)-1},a}(\beta_2)),
\end{aligned} \tag{12}$$

holds, where $\phi(\frac{\epsilon_2}{c}) = \beta_1 + \beta_2 + \phi(\epsilon_2)$.

Now, using (6) and (10), we have

$$\Gamma_{\kappa_{m(\ell)-1},\kappa_{n(\ell)-1},\kappa_{n(\ell)}}(\beta_1) \geq 1 - \lambda, \tag{13}$$

$$\Gamma_{\kappa_{m(\ell)-1},\kappa_{n(\ell)},a}(\phi(\epsilon_2)) \geq 1 - \lambda \tag{14}$$

and

$$\Gamma_{\kappa_{n(\ell)},\kappa_{n(\ell)-1},a}(\beta_2) \geq 1 - \lambda. \tag{15}$$

Since Δ is a min t-norm, using (13), (14), and (15) in (12), we have $\Gamma_{\kappa_{m(\ell)-1},\kappa_{n(\ell)-1},a}(\phi(\frac{\epsilon_2}{c})) \geq \Delta(1-\lambda, 1-\lambda, 1-\lambda) = 1-\lambda$, $\frac{1}{\Gamma_{\kappa_{m(\ell)-1},\kappa_{n(\ell)-1},a}(\phi(\frac{\epsilon_2}{c}))} \leq \frac{1}{1-\lambda}$, that is,

$$\frac{1}{\Gamma_{\kappa_{m(\ell)-1},\kappa_{n(\ell)-1},a}(\phi(\frac{\epsilon_2}{c}))} - 1 \leq \frac{1}{1-\lambda} - 1 = \frac{\lambda}{1-\lambda}. \tag{16}$$

Again, using (6), we have $\Gamma_{\kappa_{m(k)-1},\kappa_{m(\ell)},a}(\phi(\frac{\epsilon_2}{c})) \geq 1 - \lambda$, $\frac{1}{\Gamma_{\kappa_{m(\ell)-1},\kappa_{m(\ell)},a}(\phi(\frac{\epsilon_2}{c}))} \leq \frac{1}{1-\lambda}$, that is,

$$\frac{1}{\Gamma_{\kappa_{m(\ell)-1},\kappa_{m(\ell)},a}(\phi(\frac{\epsilon_2}{c}))} - 1 \leq \frac{1}{1-\lambda} - 1 = \frac{\lambda}{1-\lambda}. \tag{17}$$

Again, $\frac{1}{\Gamma_{\kappa_{n(\ell)-1},\kappa_{n(\ell)},a}(\phi(\frac{\epsilon_2}{c}))} \leq \frac{1}{1-\lambda}$, $\frac{1}{\Gamma_{\kappa_{n(\ell)-1},\kappa_{n(\ell)},a}(\phi(\frac{\epsilon_2}{c}))} \leq \frac{1}{1-\lambda}$, that is,

$$\frac{1}{\Gamma_{\kappa_{n(\ell)-1},\kappa_{n(\ell)},a}(\phi(\frac{\epsilon_2}{c}))} - 1 \leq \frac{1}{1-\lambda} - 1 = \frac{\lambda}{1-\lambda}. \tag{18}$$

Now, using (16), (17) and (18) in (11), we have

$$\begin{aligned}
\frac{\lambda}{1-\lambda} &< \min(\frac{1}{\Gam_{\kappa_{m(\ell)-1},\kappa_{n(\ell)-1},a}(\phi(\frac{\epsilon_2}{c}))} - 1, \\
&\quad \frac{1}{\Gamma_{\kappa_{m(\ell)-1},\kappa_{m(\ell)},a}(\phi(\frac{\epsilon_2}{c}))} - 1, \frac{1}{\Gamma_{\kappa_{n(\ell)-1},\kappa_{n(\ell)},a}(\phi(\frac{\epsilon_2}{c}))} - 1) \\
&\leq \min(\frac{\lambda}{1-\lambda}, \frac{\lambda}{1-\lambda}, \frac{\lambda}{1-\lambda}) \\
&= \frac{\lambda}{1-\lambda},
\end{aligned}$$

which is a contradiction. Hence $\{\kappa_n\}$ is a Cauchy sequence.
Since (S, Γ, Δ) be a complete 2-Menger space, $\kappa_n \to u$ as $n \to \infty$, for some $u \in S$. Moreover, we get

$$\Gamma_{hu,u,a}(\epsilon) \geq \Delta(\Gamma_{hu,u,\kappa_{n+1}}(\frac{\epsilon}{3}), \Gamma_{hu,\kappa_{n+1},a}(\frac{\epsilon}{3}), \Gamma_{\kappa_{n+1},u,a}(\frac{\epsilon}{3})). \tag{19}$$

Next, using the properties of function ϕ, we can find $\eta_2 > 0$ such that $\phi(\eta_2) < \frac{\epsilon}{3}$. Since $\kappa_n \to u$ as $n \to \infty$, there exists $n_0 \in N$ such that, for all $n > n_0$ (sufficiently large), we have
$\frac{1}{\Gamma_{\kappa_{n+1},hu,a}(\frac{\epsilon}{3})} - 1 \leq \frac{1}{\Gamma_{h\kappa_n,hu,a}(\phi(\eta_2))} - 1 \leq \alpha(\kappa_n, u, \eta)(\frac{1}{\Gamma_{h\kappa_n,hu,a}(\phi(\eta_2))} - 1)$
$\leq \min(\frac{1}{\Gamma_{\kappa_n,u,a}(\phi(\frac{\eta_2}{c}))} - 1, \frac{1}{\Gamma_{\kappa_n,h\kappa_n,a}(\phi(\frac{\eta_2}{c}))} - 1, \frac{1}{\Gamma_{u,hu,a}(\phi(\frac{\eta_2}{c}))} - 1)$
$= \min(\frac{1}{\Gamma_{\kappa_n,u,a}(\phi(\frac{\eta_2}{c}))} - 1, \frac{1}{\Gamma_{\kappa_n,\kappa_{n+1},a}(\phi(\frac{\eta_2}{c}))} - 1, \frac{1}{\Gamma_{u,hu,a}(\phi(\frac{\eta_2}{c}))} - 1).$

Taking limit $n \to \infty$ on both sides, we have $\frac{1}{\Gamma_{u,hu,a}(\phi(\eta_2))} - 1 \leq \min(0, 0, \frac{1}{\Gamma_{u,hu,a}(\phi(\frac{\eta_2}{c}))} - 1) = 0$. Hence $\frac{1}{\Gamma_{u,hu,a}(\phi(\eta_2))} \leq 1, \Gamma_{u,hu,a}(\phi(\eta_2)) \geq 1$. Hence $hu = u$. So, it is proved that h has a fixed point.

Now, we'll show that the uniqueness of fixed point. Let κ and μ be two fixed point of h, that is, $h\kappa = \kappa$ and $h\mu = \mu$ with $\kappa \neq \mu$. By the virtue of ϕ there exists $s > 0$ such that $\Gamma_{\kappa,\mu,a}(\phi(s)) > 0$ for all $a \in S$. Then, by (1), we have

$$\begin{aligned}
\frac{1}{\Gamma_{h\kappa,h\mu,a}(\phi(s))} - 1 &\leq \alpha(\kappa, \mu, \eta)(\frac{1}{\Gamma_{h\kappa,h\mu,a(\phi(s))}} - 1) \\
&\leq \min(\frac{1}{\Gamma_{\kappa,\mu,a}(\phi(\frac{s}{c}))} - 1, \frac{1}{\Gamma_{\kappa,h\kappa,a}(\phi(\frac{s}{c}))} - 1, \\
&\quad \frac{1}{\Gamma_{\mu,h\mu,a}(\phi(\frac{s}{c}))} - 1) \\
&= \min(\frac{1}{\Gamma_{\kappa,\mu,a}(\phi(\frac{s}{c}))} - 1, \frac{1}{\Gamma_{\kappa,\kappa,a}(\phi(\frac{s}{c}))} - 1, \\
&\quad \frac{1}{\Gamma_{\mu,\mu,a}(\phi(\frac{s}{c}))} - 1) \\
&= \min(\frac{1}{\Gamma_{\kappa,\mu,a}(\phi(\frac{s}{c}))} - 1, 0, 0) \\
&= 0.
\end{aligned}$$

Hence $\Gamma_{h\kappa,h\mu,a}(\phi(s)) \geq 1$, for all $a \in S$, and it implies $\kappa = \mu$.

If we replace $\phi(\eta)$ by t and $\alpha(\kappa, \mu, \eta) = 1$, in the above theorem, we get the following result.

Corollary 19. *Let (S, Γ, Δ) be a complete 2-Menger space and $h : S \to S$ be a mapping satisfying the following inequality for all $\kappa, \mu, a \in S$,*

$$\frac{1}{\Gamma_{h\kappa,h\mu,a}(\eta)} - 1 \leq \min(\frac{1}{\Gamma_{\kappa,\mu,a}(\frac{\eta}{c})} - 1, \frac{1}{\Gamma_{\kappa,h\kappa,a}(\frac{\eta}{c})} - 1, \frac{1}{\Gamma_{\mu,h\mu,a}(\frac{\eta}{c})} - 1) \tag{20}$$

where $\eta > 0$, $0 < c < 1$. Then h has a unique fixed point in S.

Next we give an example to support our results.

Example 20. Let $S = \{\kappa_1, \kappa_2, \kappa_3, \kappa_4\}$, the t-norm Δ is a minimum t-norm and Γ be defined as

$$\Gamma_{\kappa_1,\kappa_2,\kappa_3}(\eta) = \Gamma_{\kappa_1,\kappa_2,\kappa_4}(\eta) = \begin{cases} 0, & \text{if} \quad \eta \leq 0, \\ 0.50, & \text{if} \quad 0 < \eta \leq 5, \\ 1, & \text{if} \quad \eta > 5. \end{cases}$$

and

$$\Gamma_{\kappa_1,\kappa_3,\kappa_4}(\eta) = \Gamma_{\kappa_2,\kappa_3,\kappa_4}(\eta) = \begin{cases} 0, & \text{if} \quad \eta \leq 0, \\ 1, & \text{if} \quad \eta > 0, \end{cases}$$

Then (S, Γ, Δ) is a complete 2-Menger space. If we define $h : S \to S$ as follows: $h\kappa_1 = \kappa_4, h\kappa_2 = \kappa_3, h\kappa_3 = \kappa_4, h\kappa_4 = \kappa_4$, then the mapping h satisfies all the conditions of the theorem where $\phi(\eta) = \eta$, $c \in (0, 1)$ and $\alpha(\kappa, \mu, \eta) = 1$. Then κ_4 is the unique fixed point of h in S.

CONCLUSION

In recent research work, it is clear that contraction mappings play vital roles. The contraction is supposed to appear in probabilistic analysis also. Many researchers have concentrated their works on these spaces. Some authors also showed that PM spaces are applicable also in nuclear fusion. G. Verdoolage et. al Verdoolage et al. (2012) may be noted in this respect. The authors have showed that PM spaces have an important role to identify confinement regimes and plasma disruption. The distribution function plays the role of metric in these spaces. Also it may be noted that t-norm has an important role. Here we use the minimum t-norm. But we think that different types t-norm may be used here. These problems may be taken up as future open problems.

REFERENCES

Bhandari, S. K. 2017a, Probabilistic Ciric type contraction results using drastic t-norm, Bull. Cal. Math. Soc., 109(6), pp. 439-454.

Bhandari, S. K. 2017b, Unique Probablistic p-cyclic c-contraction results using special product T-Norm, Bull. Cal. Math. Soc., 109(1), pp. 55-68.

Bhandari, S. K. & Choudhury, B. S. 2017, Two unique fixed point results of p-cyclic probabilistic c-contractions using different types of t-norm, J. Internat. Math. Virt. Inst., 7, pp. 147-164.

Choudhury, B. S. & Bhandari, S. K. 2014, Ciric type p-cyclic contraction results for discontinuous mappings, J. Int. Math. Virt. Inst., 4, pp. 27-42.

Choudhury, B. S. & Bhandari, S. K. 2016, P- cyclic c-contraction result in Menger spaces using a control function, Demonst. Math., 49 (2), pp. 213-223. https://doi.org/10.1515/dema-2016-0018

Choudhury, B. S., Bhandari, S. K., & Saha, P. 2015, A cyclic probabilistic c-contraction results using Hadzic and Lukasiewicz t-norms Menger spaces, Anal. Theory Appl., 31, pp. 283-298.

Choudhury, B. S. & Das, K. P. 2008, A new contraction principle in Menger spaces, Acta Math. Sinica, 24, pp. 1379-1386.

Choudhury, B. S., Das, K. P., & Bhandari, S. K. 2012, Two Ciric type probabilistic fixed point theorems for discontinuous mappings, Internat. Elect. J. Pure Appl. Math., 5(3), pp. 111-126.

Dutta, P. N., Choudhury, B. S., & Das, K. P. 2009, Some fixed point results in Menger spaces using a control function, Sur. Math. Appl., 4, pp. 41-52.

G*ä*hler, S. 1963, 2-metrische R*ä*ume und ihre topologische Struktur, Math. Nachr., 26, pp. 115-148. https://doi.org/10.1002/mana.19630260109

G*ä*hler, S. 1965, Uber die unifromisieberkeit 2-metrischer Räume, Math. Nachr., 28, pp. 235-244.

Gopal, D., Abbas, M., & Vetro, C. 2014, Some new fixed point theorems in Menger PM-spaces with application to Volterra type integral equation, Appl. Math. Comput., 232, pp. 955-967. https://doi.org/10.1016/j.amc.2014.01.135

Hadzic, O. 1994, A fixed point theorem for multivalued mappings in 2-menger spaces, Univ. u Novom Sadu, Zb. Rad. Prirod. Mat. Fak., Ser. Mat., 24, pp. 1-7.

Hadzic, O. & Pap, E. 2001, Fixed Point Theory in Probabilistic Metric Spaces (Kluwer Academic Publishers).

Khan, M., Swaleh, M., & Sessa, S. 1984, Fixed point theorems by altering distances between the points, Bull. Austral. Math. Soc., 30, pp. 1-9.

Kutbi, M. A., Gopal, D., Vetro, C., & Sintunavarat, W. 2015, Further generalization of fixed point theorems in Menger PM-spaces, Fixed Point Theory Appl., 2015(32). https://doi.org/10.1186/s13663-015-0279-4

Mihet, D. 2009, Altering distances in probabilistic Menger spaces, Nonlinear Anal., 71, pp. 2734-2738.

Schweizer, B. & Sklar, A. 1983, Probabilistic Metric Spaces, Vol. Probabilistic Metric Spaces (Elsevier, North-Holland). (Elsevier, North-Holland)

Shi, Y., Ren, L., & Wang, X. 2003, The extension of fixed point theorems for set valued mapping, J. Appl. Math. Comput., 13, pp. 277-286.

Shih-sen, C. & Nan-Jing, H. 1989, On generalized 2-metric spaces and probabilistic 2-metric spaces with applications to fixed point theory, Math. Jap., 34(6), pp. 885-900.

Verdoolage, G., Karagounis, G., Murari, A., et al. 2012, Modelling fusion data in probabilistic metric spaces: applications to the identification of confinement regimes and plasma disruptions, Fusion Sci. Tech., 62(2), pp. 356-365. https://doi.org/10.13182/FST12-A14627

Zeng, W.-Z. 1987, Probabilistic 2-metric spaces, J. Math. Research Expo., 2, pp. 241-245.

Bulletin of Natural Sciences Research
Vol.12, No.1, 2022, pp. 11-14.

DOI: https://doi.org/10.5937/bnsr12-33064
Original Scientific Paper

EXISTENCE OF INVARIANT POINTS AND APPLICATIONS TO SIMULTANEOUS APPROXIMATION

SUMIT CHANDOK[1,⋆], **T. D. NARANG**[2]

[1]School of Mathematics, Thapar Institute of Engineering Technology, Patiala-147004, India.
[2]Department of Mathematics, Guru Nanak Dev University, Amritsar-143005, India

ABSTRACT

For the set of ε-simultaneous approximation and ε-simultaneous coapproximation, we derive certain Brosowski-Meinardus type invariant point results in this paper. As a consequence, some results on ε-approximation, ε-coapproximation, best approximation, and best coapproximation are also deduced.

Keywords: ε-simultaneous approximatively compact set, Starshaped set, Best approximation, Best simultaneous approximation, ε-simultaneous approximation.

INTRODUCTION AND PRELIMINARIES

The study of best approximation theory plays an important role in nonlinear functional analysis, optimization theory, fixed point theory, nonlinear programming, game theory, variational inequality, complementarity problems, and so forth. The idea of applying fixed point theorems to approximation theory was initiated in normed linear spaces by Meinardus (1963). Later, Brosowski (1969) generalized the result of Meinardus and proved a nice result on invariant approximation. Thereafter, various generalizations of Brosowski's results appeared in the literature.

Singh (1979a) observed that the linearity of the operator $\mathscr{T}$ and convexity of the set $P_{\mathcal{G}}(\mathfrak{x})$ can be relaxed and proved an interesting result. Later, Singh (1979b) demonstrated that previous result of Singh (1979a) remains valid if $\mathscr{T}$ is assumed to be nonexpansive only on the set $P_{\mathcal{G}}(\mathfrak{x})\cup\{\mathfrak{x}\}$. Thenceforth, many results have been obtained in this direction by many researchers (see Chandok (2019); Chandok & Narang (2011a,b, 2012a,b, 2013); Khan & Akbar (2009a,b); Mukherjee & Som (1985); Narang & Chandok (2009a,b,c); Rao & Mariadoss (1983) and references cited therein).

In this article, we obtain some similar types of results on $\mathscr{T}$-invariant points for the set of ε-simultaneous approximation and ε-simultaneous coapproximation for a Hardy-Roger type contraction mapping defined on a Takahashi space $(\mathscr{X}, d, W)$. For such class of mappings, we also deduce some results on $\mathscr{T}$-invariant points for the set of ε-approximation, ε-coapproximation, best approximation and best coapproximation.

Definition 1. Let $(\mathscr{X}, d)$ be a metric space, $\emptyset \neq \mathcal{G} \subset \mathscr{X}$, $\mathcal{F}$ a nonempty bounded subset of $\mathscr{X}$. For $\mathfrak{x} \in \mathscr{X}$, assume that

$$d_{\mathcal{F}}(\mathfrak{x}) = \{\sup d(y, \mathfrak{x}) : y \in \mathcal{F}\},$$
$$D(\mathcal{F}, \mathcal{G}) = \{\inf d_{\mathcal{F}}(\mathfrak{x}) : \mathfrak{x} \in \mathcal{G}\},$$
and
$$P_{\mathcal{G}}(\mathcal{F}) = \{g_0 \in \mathcal{G} : d_{\mathcal{F}}(g_0) = D(\mathcal{F}, \mathcal{G})\}.$$

An element $g_0 \in P_{\mathcal{G}}(\mathcal{F})$ is said to be a **best simultaneous approximation** of $\mathcal{F}$ with respect to $\mathcal{G}$ (see Chandok & Narang (2011a)).

For $\varepsilon > 0$, we define

$$\begin{aligned} P_{\mathcal{G}(\varepsilon)}(\mathcal{F}) =& \{g_0 \in \mathcal{G} : d_{\mathcal{F}}(g_0) \leq D(\mathcal{F}, \mathcal{G}) + \varepsilon\} \\ =& \{g_0 \in \mathcal{G} : \sup_{y\in\mathcal{F}} d(y, g_0) \leq \inf_{g\in\mathcal{G}} \sup_{y\in\mathcal{F}} d(y, g) + \varepsilon\}. \end{aligned}$$

An element $g_0 \in P_{\mathcal{G}(\varepsilon)}(\mathcal{F})$ is said to be a ε-simultaneous approximation of $\mathcal{F}$ with respect to $\mathcal{G}$ (see Chandok & Narang (2011a)).

It can be easily seen that for $\varepsilon > 0$, the set $P_{\mathcal{G}}(\varepsilon)(\mathcal{F})$ is always a nonempty bounded set and is closed if $\mathcal{G}$ is closed.

In case $\mathcal{F} = \{p\}$, $p \in \mathscr{X}$, then elements of $P_{\mathcal{G}}(p)$ are called **best approximations** to p in $\mathcal{G}$ and of $P_{\mathcal{G}(\varepsilon)}(p)$ are called ε-**approximation** to p in $\mathcal{G}$.

For $\varepsilon > 0$, we define

$$R_{\mathcal{G}(\varepsilon)}(\mathcal{F}) = \{g_0 \in \mathcal{G} : \sup_{g\in\mathcal{G}} d(g_0, g) + \varepsilon \leq \inf_{g\in\mathcal{G}} \sup_{y\in\mathcal{F}} d(y, g)\}.$$

An element $g_0 \in R_{\mathcal{G}(\varepsilon)}(\mathcal{F})$ is said to be a ε-simultaneous coapproximation of $\mathcal{F}$ with respect to $\mathcal{G}$ (see Chandok & Narang (2011a)).

In case $\mathcal{F} = \{p\}$, $p \in \mathscr{X}$, then elements of $R_{\mathcal{G}}(p)$ are called **best coapproximations** to p in $\mathcal{G}$ and of $R_{\mathcal{G}(\varepsilon)}(p)$ are called ε-**coapproximation** to p in $\mathcal{G}$.

Let $\mathscr{T}$ be a self mapping defined on a subset $\mathcal{G}$ of a metric space $\mathscr{X}$. A best approximant $\mathfrak{y}$ in $\mathcal{G}$ to an element $\mathfrak{x}_0$ in $\mathscr{X}$ with $\mathscr{T}\mathfrak{x}_0 = \mathfrak{x}_0$ is an invariant approximation in $\mathscr{X}$ to $\mathfrak{x}_0$ if $\mathscr{T}\mathfrak{y} = \mathfrak{y}$.

Example 2. Let $\mathscr{X} = \mathbb{R}$ with usual metric and $\mathcal{G} = [0, 1] \subset \mathscr{X}$. Define $\mathscr{T} : \mathscr{X} \to \mathscr{X}$ as

$$\mathscr{T}\mathfrak{x} = \begin{cases} \mathfrak{x}, \mathfrak{x} < 2 \\ \frac{\mathfrak{x}+2}{2}, \mathfrak{x} \geq 2. \end{cases}$$

Clearly, $\mathscr{T}(\mathcal{G}) = \mathcal{G}$ and $\mathscr{T}(2) = 2$. Also, $P_{\mathcal{G}}(2) = \{1\}$. Hence $\mathscr{T}$ has a fixed point in $\mathscr{X}$ which is a best approximation to 2 in $\mathcal{G}$. Thus, 2 is an invariant approximation.

⋆ Corresponding author: sumit.chandok@thapar.edu

Definition 3. A sequence $\{y_n\}$ in $\mathcal{G}$ is called a ε-**minimizing sequence** for $\mathcal{F}$, if

$$\limsup_{x\in\mathcal{F}} d(x, y_n) \leq D(\mathcal{F}, \mathcal{G}) + \varepsilon.$$

The set $\mathcal{G}$ is said to be ε-**simultaneous approximatively compact with respect to** $\mathcal{F}$ (see Chandok & Narang (2011a)) if for every $x \in \mathcal{F}$, each ε-minimizing sequence $\{y_n\}$ in $\mathcal{G}$ has a subsequence $\{y_{n_i}\}$ converging to an element of $\mathcal{G}$.

Inspired by the work of Takahashi (1970) and Guay et al. (1982), we have the following definition.

Definition 4. Let $\mathcal{X}$ be a nonempty set, d be a metric on $\mathcal{X}$ and $W : \mathcal{X} \times \mathcal{X} \times [0, 1] \to \mathcal{X}$ be a continuous mapping satisfying, for all $x, y, u \in \mathcal{X}$ and $\lambda \in [0, 1]$,

1. $d(u, W(x, y, \lambda)) \leq \lambda d(u, x) + (1 - \lambda)d(u, y)$,
2. $d(W(x, u, \lambda), W(y, u, \lambda)) \leq d(x, y)$.

Then the triple $(\mathcal{X}, d, W)$ is called a **Takahashi space**.

A normed linear space and each of its convex subset are simple examples of Takahashi spaces with W given by $W(x, y, \lambda) = \lambda x + (1 - \lambda)y$ for $x, y \in \mathcal{X}$ and $0 \leq \lambda \leq 1$. For definition of convex set, q-starshaped set and starshaped set see Chandok & Narang (2011a) and references cited therein.

Definition 5. Let $\mathcal{G}$ be a nonempty subset of a metric space $(\mathcal{X}, d)$ and $\mathcal{T} : \mathcal{G} \to \mathcal{G}$ be a self map. Then $\mathcal{T}$ is said to be **asymptotically regular** (see, Browder & Petryshyn (1966)) if for all $x \in \mathcal{G}$, $d(\mathcal{T}^n(x), \mathcal{T}^{n+1}(x)) \to 0$ as $n \to \infty$.

Definition 6. A mapping $\mathcal{T} : \mathcal{X} \to \mathcal{X}$ satisfies **condition (A)** (see Mukherjee & Verma (1989)) if

$$d(\mathcal{T}^n x, y) \leq d(x, y),$$

for all $x, y \in \mathcal{X}$ and for some positive integer n.

MAIN RESULTS

Inspired by the work of Hardy-Roger, we define the following contraction:

Definition 7. Let $(\mathcal{X}, d)$ be a metric space. A mapping $\mathcal{T} : \mathcal{X} \to \mathcal{X}$ is called a **HR-type contraction** if there exist $\alpha, \beta, \gamma \in [0, 1)$ with $\alpha + \beta + 2\gamma < 1$, $\alpha + \gamma \neq 1$ such that for all $x, y \in \mathcal{X}$, we have

$$\begin{aligned} d(\mathcal{T}x, \mathcal{T}y) \quad \leq \quad & \alpha \frac{d(x, \mathcal{T}x)d(y, \mathcal{T}y)}{1 + d(x, y)} + \beta(d(x, y)) + \\ & \gamma(d(x, \mathcal{T}x) + d(y, \mathcal{T}y)). \end{aligned} \tag{1}$$

Remark 8. On a metric space, every HR-type contraction has at most one fixed point. Indeed, let x and y be two distinct fixed points of $\mathcal{T}$, which is a HR-type contraction. Then

$$\begin{aligned} d(x, y) = d(\mathcal{T}x, \mathcal{T}y) \quad \leq \quad & \alpha \frac{d(x, \mathcal{T}x)d(y, \mathcal{T}y)}{1 + d(x, y)} + \beta(d(x, y)) + \\ & \gamma(d(x, \mathcal{T}x) + d(y, \mathcal{T}y)) \\ = \quad & \beta(d(x, y)), \end{aligned}$$

which is a contradiction as $0 \leq \beta < 1$ and $d(x, y) > 0$.

The following result will be needed in the sequel.

Proposition 9. *Let $\mathcal{T} : \mathcal{X} \to \mathcal{X}$ be a HR-type contraction on a metric space $(\mathcal{X}, d)$. Then for all $x \in \mathcal{X}$, the sequence $\{d(\mathcal{T}^n x, \mathcal{T}^{n+1}x)\}$ is decreasing and $\mathcal{T}$ is asymptotically regular.*

Proof. Let x_0 be an arbitrary point in $\mathcal{X}$ and $\{x_n\}$ be sequence in $\mathcal{X}$ such that $x_{n+1} = \mathcal{T}x_n = \mathcal{T}^n x_0$, for every $n \geq 0$. Using (1), we have

$$\begin{aligned} d(x_{n+2}, x_{n+1}) \quad = \quad & d(\mathcal{T}x_{n+1}, \mathcal{T}x_n) \\ \leq \quad & \alpha \frac{d(x_{n+1}, \mathcal{T}x_{n+1})d(x_n, \mathcal{T}x_n)}{1 + d(x_{n+1}, x_n)} + \beta(d(x_{n+1}, x_n)) + \\ & \gamma(d(x_{n+1}, \mathcal{T}x_{n+1}) + d(x_n, \mathcal{T}x_n)) \\ = \quad & \alpha \frac{d(x_{n+1}, x_{n+2})d(x_n, x_{n+1})}{1 + d(x_{n+1}, x_n)} + \beta(d(x_{n+1}, x_n)) + \\ & \gamma(d(x_{n+1}, x_{n+2}) + d(x_n, x_{n+1})) \\ \leq \quad & (\alpha + \gamma)d(x_{n+1}, x_{n+2}) + (\beta + \gamma)d(x_{n+1}, x_n). \end{aligned}$$

This implies

$$d(x_{n+2}, x_{n+1}) \leq \frac{\beta + \gamma}{1 - \alpha - \gamma} d(x_{n+1}, x_n). \tag{2}$$

Since $L = \frac{\beta+\gamma}{1-\alpha-\gamma} < 1$, the sequence $\{d(\mathcal{T}^n x_0, \mathcal{T}^{n+1}x_0)\}$ is a decreasing sequence. Using mathematical induction, we have

$$d(x_{n+2}, x_{n+1}) \leq (L)^{n+1} d(x_1, x_0). \tag{3}$$

Taking the limit $n \to \infty$, we have $d(x_{n+2}, x_{n+1}) \to 0$, that is, $d(\mathcal{T}^n x_0, \mathcal{T}^{n+1}x_0) \to 0$. Hence the result.

Using the above proposition, we prove the following:

Theorem 10. *Every HR-type contraction on a complete metric space has unique fixed point.*

Proof. Using Proposition , the sequence $\{d(\mathcal{T}^n x_0, \mathcal{T}^{n+1}x_0)\}$ is decreasing and $d(\mathcal{T}^n x_0, \mathcal{T}^{n+1}x_0) \to 0$ as $n \to \infty$ for all $x_0 \in \mathcal{X}$. We claim that $\{x_n\}$ is a Cauchy sequence. For $m > n$, and $L = \frac{\beta + \gamma}{1 - \alpha - \gamma} < 1$ we have

$$\begin{aligned} d(x_n, x_m) &\leq d(x_n, x_{n+1}) + d(x_{n+1}, x_{n+2}) + \ldots + d(x_{m-1}, x_m) \\ &\leq (L^n + L^{n+1} + \ldots + L^{m-1})d(x_0, x_1) \\ &\leq \frac{L^n(1 - L^{m-n})}{1 - L} d(x_0, x_1). \end{aligned}$$

Therefore, $d(x_m, x_n) \to 0$, when $m, n \to \infty$. Thus $\{x_n\}$ is a Cauchy sequence in a complete metric space $\mathcal{X}$ and so there exists $u \in \mathcal{X}$ such that $\lim_{n\to\infty} x_n = u$.

Now, we'll show that the point u is a fixed point of $\mathcal{T}$. On the contrary, suppose that $\mathcal{T}u \neq u$, then $d(u, \mathcal{T}u) > 0$. Consider

$$\begin{aligned} d(x_{n+1}, \mathcal{T}u) = & d(\mathcal{T}x_n, \mathcal{T}u) \leq \alpha \frac{d(x_n, \mathcal{T}x_n)d(u, \mathcal{T}u)}{1 + d(x_n, u)} + \beta(d(x_n, u)) + \\ & \gamma(d(x_n, \mathcal{T}x_n) + d(u, \mathcal{T}u)) \\ = & \alpha \frac{d(x_n, x_{n+1})d(u, \mathcal{T}u)}{1 + d(x_n, u)} + \beta(d(x_n, u)) + \\ & \gamma(d(x_n, x_{n+1}) + d(u, \mathcal{T}u)). \end{aligned}$$

Taking $n \to \infty$, we have $d(u, \mathscr{T}u) \leq \gamma d(u, \mathscr{T}u)$, it implies that $d(u, \mathscr{T}u) = 0$. Hence u is a fixed point of $\mathscr{T}$. Using Remark , we obtain that $\mathscr{T}$ has unique fixed point.

Example 11. Let $\mathscr{X} = [0, 1]$ and d be the usual metric on $\mathscr{X}$. Define $\mathscr{T} : \mathscr{X} \to \mathscr{X}$ as $\mathscr{T}\mathfrak{x} = \begin{cases} \frac{\mathfrak{x}}{10}, & \mathfrak{x} \in [0, \frac{1}{2}] \\ \frac{\mathfrak{x}}{5} - \frac{1}{20}, & \mathfrak{x} \in (\frac{1}{2}, 1]. \end{cases}$

Suppose $\alpha = \frac{1}{8}, \beta = \frac{1}{4}, \gamma = \frac{1}{8} \in [0, 1)$ with $\alpha + \beta + 2\gamma = \frac{5}{8} < 1$. We may check that

$$d(\mathscr{T}\mathfrak{x}, \mathscr{T}y) \leq \frac{1}{8}\frac{d(\mathfrak{x}, \mathscr{T}\mathfrak{x})d(y, \mathscr{T}y)}{1 + d(\mathfrak{x}, y)} + \frac{1}{4}(d(\mathfrak{x}, y)) + \frac{1}{8}(d(\mathfrak{x}, \mathscr{T}\mathfrak{x}) + d(y, \mathscr{T}y)),$$

for all $\mathfrak{x}, y \in \mathscr{X}$. Thus using Theorem , $\mathscr{T}$ has unique fixed point. Notice that $0 \in \mathscr{X}$ is the fixed point of $\mathscr{T}$.

Theorem 12. *Let $(\mathscr{X}, d, W)$ be a complete Takahashi space, G be a nonempty subset of $\mathscr{X}$ and $\mathcal{F}$ a nonempty bounded subset of $\mathscr{X}$. Suppose that $\mathscr{T}_n$ is a self map on $P_{\mathcal{G}(\varepsilon)}(\mathcal{F})$ such that $\mathfrak{x}_{n+1} = \mathscr{T}_n\mathfrak{x} = W(\mathscr{T}^n\mathfrak{x}, q, \lambda_n)$, where $\lambda_n \in (0, 1)$ and satisfying the following for some positive integer n,*

$$\begin{aligned} d(\mathscr{T}^n\mathfrak{x}, \mathscr{T}^n y) \quad \leq \quad & \alpha\left(\frac{dist(\mathfrak{x}, [\mathscr{T}^n\mathfrak{x}, q])dist(y, [\mathscr{T}^n y, q])}{1 + d(\mathfrak{x}, y)}\right) + \\ & \beta(d(\mathfrak{x}, y)) + \\ & \gamma(dist(\mathfrak{x}, [\mathscr{T}^n\mathfrak{x}, q]) + dist(y, [\mathscr{T}^n y, q])), \end{aligned} \tag{4}$$

for all $\mathfrak{x}, y, q \in \mathscr{X}$, where $\alpha, \beta, \gamma \in [0, 1)$ with $\alpha + \beta + 2\gamma < 1$, $\alpha + \gamma \neq 1$. If $\mathscr{T}$ is continuous and $P_{\mathcal{G}(\varepsilon)}(\mathcal{F})$ is compact, and q-starshaped, then it contains a $\mathscr{T}$-invariant point.

Proof. Define $\mathscr{T}_n : P_{\mathcal{G}(\varepsilon)}(\mathcal{F}) \to P_{\mathcal{G}(\varepsilon)}(\mathcal{F})$ as $\mathscr{T}_n z = W(\mathscr{T}^n z, q, \lambda_n)$, $z \in P_{\mathcal{G}(\varepsilon)}(\mathcal{F})$ where $\{\lambda_n\}$ is a sequence in $(0, 1)$ such that $\lambda_n \to 1$. Consider

$$\begin{aligned} d(\mathscr{T}_n z, \mathscr{T}_n y) &= d(W(\mathscr{T}^n z, q, \lambda_n), W(\mathscr{T}^n y, q, \lambda_n)) \\ &\leq \lambda_n d(\mathscr{T}^n z, \mathscr{T}^n y) \\ &\leq \lambda_n\Big[\alpha\Big(\frac{d(z, [\mathscr{T}^n z, q])d(y, [\mathscr{T}^n y, q])}{1 + d(z, y)}\Big) + \beta(d(z, y)) + \\ &\quad \gamma(d(z, [\mathscr{T}^n z, q]) + d(y, [\mathscr{T}^n y, q]))\Big] \\ &\leq \lambda_n\Big[\alpha\Big(\frac{d(z, \mathscr{T}_n z)d(y, \mathscr{T}_n y)}{1 + d(z, y)}\Big) + \beta(d(z, y)) + \\ &\quad \gamma(d(z, \mathscr{T}_n z) + d(y, \mathscr{T}_n y))\Big], \end{aligned}$$

where $\lambda_n(\alpha + \beta + 2\gamma) < 1, z, y \in P_{\mathcal{G}(\varepsilon)}(\mathcal{F})$. Therefore by Theorem , each $\mathscr{T}_n$ has a unique fixed point z_n in $P_{\mathcal{G}(\varepsilon)}(\mathcal{F})$. Since $\{\mathscr{T}^n z_n\}$ is a sequence in the compact set $P_{\mathcal{G}(\varepsilon)}(\mathcal{F})$, there exists a subsequence $\{\mathscr{T}^{n_i} z_{n_i}\}$ of $\{\mathscr{T}^n z_n\}$ such that $\{\mathscr{T}^{n_i} z_{n_i}\} \to z \in P_{\mathcal{G}(\varepsilon)}(\mathcal{F})$. Moreover,

$$z_{n_i} = \mathscr{T}_{n_i} z_{n_i} = W[\mathscr{T}^{n_i} z_{n_i}, q, \lambda_{n_i}] \to z.$$

As $\mathscr{T}$ is continuous, $\mathscr{T}^{n_i} z_{n_i} \to \mathscr{T}^{n_i} z$. By the uniqueness of the limit, we have $\lim_{n\to\infty} \mathscr{T}^{n_i} z = z$ and so $\lim_{n\to\infty} \mathscr{T}^{n_i+1} z = \mathscr{T}z$.

Now, we show that $d(z, \mathscr{T}z) = 0$. Consider

$$d(z, \mathscr{T}z) \leq d(z, \mathscr{T}^{n_i} z) + d(\mathscr{T}^{n_i} z, \mathscr{T}^{n_i+1} z) + d(\mathscr{T}^{n_i+1} z, \mathscr{T}z).$$

Letting $n \to \infty$, in the above inequality, and using $\mathscr{T}$ is asymptotically regular, we have $d(z, \mathscr{T}z) \to 0$. Therefore $\mathscr{T}z = z$. i.e. z is $\mathscr{T}$-invariant.

Using Proposition 2.1 of Chandok & Narang (2011a), we have the following result.

Corollary 13. *Let $(\mathscr{X}, d, W)$ be a complete Takahashi space, G be a nonempty subset of $\mathscr{X}$ and $\mathcal{F}$ a nonempty bounded subset of $\mathscr{X}$. Suppose that $\mathscr{T}_n$ is a self map on $P_{\mathcal{G}(\varepsilon)}(\mathcal{F})$ such that $\mathfrak{x}_{n+1} = \mathscr{T}_n\mathfrak{x} = W(\mathscr{T}^n\mathfrak{x}, q, \lambda_n)$, where $\lambda_n \in (0, 1)$ and satisfying the inequality* (4)*. If $\mathscr{T}$ is continuous, $\mathcal{G}$ is ε-simultaneous approximatively compact with respect to $\mathcal{F}$ and $P_{\mathcal{G}(\varepsilon)}(\mathcal{F})$ is starshaped, then it contains a $\mathscr{T}$-invariant point.*

For $\mathcal{F} = \{\mathfrak{x}\}$ and $\varepsilon = 0$, we have the following result on the set of best approximation.

Corollary 14. *Let $(\mathscr{X}, d, W)$ be a complete Takahashi space, G be a nonempty subset of $\mathscr{X}$. Suppose that $\mathscr{T}_n$ is a self map on $P_{\mathcal{G}(\varepsilon)}(\mathcal{F})$ such that $\mathfrak{x}_{n+1} = \mathscr{T}_n\mathfrak{x} = W(\mathscr{T}^n\mathfrak{x}, q, \lambda_n)$, where $\lambda_n \in (0, 1)$ and satisfying the inequality* (4)*. If $\mathscr{T}$ is continuous, $\mathcal{G}$ is approximatively compact, $\mathscr{T}$-invariant subset of $\mathscr{X}$ and $\mathfrak{x}$ a $\mathscr{T}$-invariant point and $P_{\mathcal{G}}(\mathfrak{x})$ is starshaped, then $P_{\mathcal{G}}(\mathfrak{x})$ contains a $\mathscr{T}$-invariant point.*

We now prove a result for $\mathscr{T}$-invariant points from the set of ε-simultaneous coapproximations.

Theorem 15. *Let $(\mathscr{X}, d, W)$ be a complete Takahashi space, G be a nonempty subset of $\mathscr{X}$ and $\mathcal{F}$ a nonempty bounded subset of $\mathscr{X}$. Suppose that $\mathscr{T}_n$ is a self map on $R_{\mathcal{G}(\varepsilon)}(\mathcal{F})$ such that $\mathfrak{x}_{n+1} = \mathscr{T}_n\mathfrak{x} = W(\mathscr{T}^n\mathfrak{x}, q, \lambda_n)$, where $\lambda_n \in (0, 1)$ and satisfying the inequality* (4)*. Assume that $\mathscr{T}$ is continuous and satisfying condition (A). If $R_{\mathcal{G}(\varepsilon)}(\mathcal{F})$ is compact and q-starshaped, then $R_{\mathcal{G}(\varepsilon)}(\mathcal{F})$ contains a $\mathscr{T}$-invariant point.*

Proof. Let $g_0 \in R_{\mathcal{G}(\varepsilon)}(\mathcal{F})$. Consider

$$d(\mathscr{T}^n g_0, g) + \varepsilon \leq d(g_0, g) + \varepsilon \leq \inf_{g\in\mathcal{G}} sup_{y\in\mathcal{F}} d(y, g),$$

and so $\mathscr{T}^n g_0 \in R_{\mathcal{G}(\varepsilon)}(\mathcal{F})$ i.e. $\mathscr{T}^n : R_{\mathcal{G}(\varepsilon)}(\mathcal{F}) \to R_{\mathcal{G}(\varepsilon)}(\mathcal{F})$. Since $R_{\mathcal{G}(\varepsilon)}(\mathcal{F})$ is q-starshaped, $W(z, q, \lambda) \in R_{\mathcal{G}(\varepsilon)}(\mathcal{F})$ for all $z \in R_{\mathcal{G}(\varepsilon)}(\mathcal{F})$, $\lambda \in [0, 1]$. Let $\{\lambda_n\}$, $0 \leq \lambda_n < 1$, be a sequence of real numbers such that $\lambda_n \to 1$ as $n \to \infty$. Define $\mathscr{T}_n$ as $\mathscr{T}_n(z) = W(\mathscr{T}^n z, q, \lambda_n)$, $z \in R_{\mathcal{G}(\varepsilon)}(\mathcal{F})$. Since $\mathscr{T}$ is a self mapping on $R_{\mathcal{G}(\varepsilon)}(\mathcal{F})$ and $R_{\mathcal{G}(\varepsilon)}(\mathcal{F})$ is starshaped, each $\mathscr{T}_n$ is a well defined

and maps $R_{\mathcal{G}(\varepsilon)}(\mathcal{F})$ into $R_{\mathcal{G}(\varepsilon)}(\mathcal{F})$. Moreover,

$$\begin{aligned} d(\mathscr{T}_n y, \mathscr{T}_n z) &= d(W(\mathscr{T}^n y, q, \lambda_n), W(\mathscr{T}^n z, q, \lambda_n)) \\ &\leq \lambda_n d(\mathscr{T}^n y, \mathscr{T}^n z) \\ &\leq \lambda_n \Big[\alpha\Big(\frac{d(y, [\mathscr{T}^n y, q])d(z, [\mathscr{T}^n z, q])}{1 + d(y, z)}\Big) + \beta(d(y, z)) + \\ &\quad \gamma(d(y, [\mathscr{T}^n y, q]) + d(z, [\mathscr{T}^n z, q]))\Big] \\ &\leq \lambda_n \Big[\alpha\Big(\frac{d(y, \mathscr{T}^n y)d(z, \mathscr{T}^n z)}{1 + d(y, z)}\Big) + \beta(d(y, z)) + \\ &\quad \gamma(d(y, \mathscr{T}^n y)d(z, \mathscr{T}^n z))\Big], \end{aligned}$$

where $\lambda_n[\alpha + \beta] < 1$. So by Theorem each $\mathscr{T}_n$ has a unique fixed point $u_n \in R_{\mathcal{G}(\varepsilon)}(\mathcal{F})$ i.e. $\mathscr{T}_n u_n = u_n$ for each n. Since $\{\mathscr{T}^n u_n\}$ is a sequence in the compact set $R_{\mathcal{G}(\varepsilon)}(\mathcal{F})$, there exists a subsequence $\{\mathscr{T}^{n_i} u_{n_i}\}$ of $\{\mathscr{T}^n u_n\}$ such that $\{\mathscr{T}^{n_i} u_{n_i}\} \to u \in R_{\mathcal{G}(\varepsilon)}(\mathcal{F})$. Moreover,

$$u_{n_i} = \mathscr{T}_{n_i} u_{n_i} = W[\mathscr{T}^{n_i} u_{n_i}, q, \lambda_{n_i}] \to u.$$

As $\mathscr{T}$ is continuous, $\mathscr{T}^{n_i} u_{n_i} \to \mathscr{T}^{n_i} u$. By the uniqueness of the limit, we have $\lim_{n\to\infty} \mathscr{T}^{n_i} u = u$ and so $\lim_{n\to\infty} \mathscr{T}^{n_i+1} u = \mathscr{T} u$.

Now, we show that $d(u, \mathscr{T} u) = 0$. Since $\mathscr{T}$ is asymptotically regular, we have

$$d(u, \mathscr{T} u) \leq d(u, \mathscr{T}^{n_i} u) + d(\mathscr{T}^{n_i} u, \mathscr{T}^{n_i+1} u) + d(\mathscr{T}^{n_i+1} u, \mathscr{T} u) \to 0.$$

Therefore $\mathscr{T} u = u$. i.e. u is $\mathscr{T}$-invariant.

Remark 16.

1. By taking $\mathcal{F} = \{\mathfrak{x}_1, \mathfrak{x}_2\}$, $\mathfrak{x}_1, \mathfrak{x}_2 \in \mathscr{X}$, the set $P_{\mathcal{G}(\varepsilon)}(\mathcal{F})$ (respectively, $R_{\mathcal{G}(\varepsilon)}(\mathcal{F})$) is the set of ε-simultaneous approximation (respectively, ε-simultaneous coapproximation) to the pair of points $\mathfrak{x}_1, \mathfrak{x}_2$ and so we can obtain the results for such pair of points $P_{\mathcal{G}(\varepsilon)}(\mathcal{F})$ (respectively, $R_{\mathcal{G}(\varepsilon)}(\mathcal{F})$).
2. By taking $\mathcal{F} = \{\mathfrak{x}\}$, $\mathfrak{x} \in \mathscr{X}$, the set $P_{\mathcal{G}(\varepsilon)}(\mathfrak{x})$ (respectively, $R_{\mathcal{G}(\varepsilon)}(\mathfrak{x})$) is the set of ε-approximation(respectively, ε-coapproximation) to point $\mathfrak{x}$ and so we can obtain the results on the set of ε-approximation (respectively, ε-coapproximation).
3. By taking $\mathcal{F} = \{\mathfrak{x}\}$ and $\varepsilon = 0$, we can obtain the results on the set of best approximation (respectively, best coapproximation).

REFERENCES

Brosowski, B. 1969, Fixpunktsätze in der Approximationstheorie, Mathematica (Cluj), 11, pp. 195-200.

Browder, F. E. & Petryshyn, W. V. 1966, The solution by iteration of nonlinear functional equations in Banach spaces, Bull. Amer. Math. Soc., 72, pp. 571-5775.

Chandok, S. 2019, Best approximation and fixed points for rational-type contraction mappings, J. Appl. Anal., 25(2), pp. 205-209. https://doi.org/10.1515/jaa-2019-0021

Chandok, S. & Narang, T. 2011a, Invariant points and ε-simultaneous approximation, Internat. J. Math. Math. Sci., 2011 (579819). doi:10.1155/2011/579819

Chandok, S. & Narang, T. 2011b, ε-simultaneous approximation and invariant points, Bull. Belgian Math. Soc., 18, pp. 821-834. https://doi.org/10.36045/bbms/1323787169

Chandok, S. & Narang, T. D. 2012a, Common fixed points of nonexpansive mappings with applications to best and best simultaneous approximation, J. Appl. Anal., 18, pp. 33-46.

Chandok, S. & Narang, T. D. 2012b, Common fixed points with applications to best simultaneous approximations, Anal. Theory Appl., 28(1), pp. 1-12. https://doi.org/10.1515/jaa-2012-0002

Chandok, S. & Narang, T. D. 2013, Some fixed point theorem for generalized asymptotically nonexpansive mapping, Tamkang J. Math., 44(1), pp. 23-29. https://doi.org/10.5556/j.tkjm.44.2013.898

Guay, M. D., Singh, K. L., & Whitfield, J. H. M. 1982, Fixed point theorems for nonexpansive mappings in convex metric spaces, Proc. Conference on nonlinear analysis (Ed. S.P. Singh and J.H. Bury) Marcel Dekker, 80, pp. 179-189.

Khan, A. R. & Akbar, F. 2009a, Best simultaneous approximations, asymptotically nonexpansive mappings and variational inequalities in Banach spaces, J. Math. Anal. Appl., 354, pp. 469-477. https://doi.org/10.1016/j.jmaa.2009.01.007

Khan, A. R. & Akbar, F. 2009b, Common fixed points from best simultaneous approximation, Taiwanese J. Math., 13, pp. 1379-1386. doi:10.11650/twjm/1500405546

Meinardus, G. 1963, Invarianz bei linearen Approximationen, Arch. Rational Mech. Anal., 14, pp. 301-303.

Mukherjee, R. N. & Som, T. 1985, A note on application of a fixed point theorem in approximation theory, Indian J. Pure Appl. Math., 16, pp. 243-244.

Mukherjee, R. N. & Verma, V. 1989, Best approximations and fixed points of nonexpansive maps, Bull. Cal. Math. Soc., 81, pp. 191-196.

Narang, T. D. & Chandok, S. 2009a, Fixed points and best approximation in metric spaces, Indian J. Math., 51, pp. 293-303.

Narang, T. D. & Chandok, S. 2009b, Fixed points of quasinonexpansive mappings and best approximation, Selcuk J. Appl. Math., 10, pp. 75-80.

Narang, T. D. & Chandok, S. 2009c, On ε-approximation and fixed points of nonexpansive mappings in metric spaces, Mat. Vesnik, 61, pp. 165-171.

Rao, G. S. & Mariadoss, S. A. 1983, Applications of fixed point theorems to best approximations, Serdica-Bulgaricae Math. Publ., 9, pp. 244-248.

Singh, S. P. 1979a, An application of a fixed-point theorem to approximation theory, J. Approx. Theory, 25, pp. 89-90.

Singh, S. P. 1979b, Application of fixed point theorems in approximation theory, Appl. Nonlinear Anal. (Ed. V. Lakshmikantham), Academic Press, New York, pp. 389-397.

Takahashi, W. 1970, A convexity in metric space and nonexpansive mappings I, Kodai Math. Sem. Rep., 22, pp. 142-149.

Bulletin of Natural Sciences Research
Vol. 12, No. 1, 2022, pp. 15-20.

DOI: https://doi.org/10.5937/bnsr12-38771
Original Scientific Paper

SPECTRAL CHARACTERISTICS OF TWO PARAMETER FIFTH DEGREE POLYNOMIAL CONVOLUTION KERNEL

ZORAN MILIVOJEVIĆ[1], NATAŠA SAVIĆ[1], BOJAN PRLINČEVIĆ[2*]

[1]Academy of Applied Technical and Preschool Studies, Niš, Serbia
[2]Kosovo and Metohija Academy of Applied Studies, Leposavić, Serbia

ABSTRACT

In this paper, the spectral characteristic of a polynomial two parameter convolutional fifth - order interpolation kernel is determined. The spectral characteristic is determined as follows. First, the kernel is decomposed into components. After that, the spectral characteristics of each kernel component were calculated using the Fourier transform. Finally, the spectral characteristic of the interpolation two parameter kernel using a combination of the spectral components of the kernels and the kernel parameters, α and β, is formed. Through a numerical example and a graphical representation of the spectral characteristics of the one parameter and two parameter kernels, greater similarity of the spectral characteristics of the 2 P kernel, relative to the ideal box characteristic, is shown.

Keywords: Convolution, Interpolation, PCC interpolation, Polynomial kernel.

INTRODUCTION

Theoretical analyzes of convolutional interpolation have shown that, for interpolation of band limited signals, the interpolation kernel $sin(x) / x$ (in the notation *sinc*) should be applied (Keys, 1981). The *sinc* interpolation kernel is called the ideal interpolation kernel. he boundaries of the *sinc* interpolation kernel are $-\infty \leq x \leq +\infty$ (Meijering & Unser, 2003). The spectral characteristic of the *sinc* interpolation kernel is a rectangular or, in some notations, box function. From a practical point of view, it is not possible to implement a kernel with boundaries $-\infty \leq x \leq +\infty$. The solution to this problem was found in the truncated sinc kernel, so that the kernel becomes a finite length L. The process of truncated the kernel to finite length is called windowizing (Dodgson, 1997). Truncated distinguishes the spectral characteristic of the interpolation kernel from the ideal spectral characteristic, ie from the box characteristic. The spectral characteristics of the truncated kernel, *sincw*, have: a) ripple in the passband and stopband, and b) finite slope in the transition band.

In order to reduce the numerical complexity of the interpolation kernel, and thus reduce the interpolation time, approximation of the *sinc* kernel with low-degree polynomial functions is performed. Reducing of the interpolation time is especially important for convolutional interpolation in real-time systems. A zero-degree polynomial kernel performs nearest-neighbor interpolation (Dodgson, 1997). The nearest-neighbor interpolation has a very high computational speed. However, a large interpolation error is generated (Rukundo & Maharaj, 2014).

A linear, first-degree interpolation kernel is described in (Rifman, 1973). A quadratic, second-degree interpolation kernel is described in (Dodgson, 1997) and (Deng, 2010). A cubic, third-degree interpolation kernel is described in (Keys, 1981). Detailed numerical analysis of the interpolation error, which is presented in great detail in (Keys, 1981), showed that the interpolation error, when the cubic kernel was applied, is smaller than the interpolation errors when the nearest-neighbor and linear interpolation kernels were applied. Thus, precision, as one of the parameters for estimating the quality of interpolation, is increased.

A cubic kernel with interpolation parameter α is shown in (Keys, 1981). Later, in the scientific literature, the one parametric interpolation kernel from (Keys, 1981), in honor of the author Roberts B. Keys, the 1P Keys interpolation kernel, was named. By adjusting of the parameter α it is possible to minimize of the interpolation error in various applications (image interpolation, audio signal interpolation, etc.) The process of changing the kernel parameter for customization is called parameter optimization. Changing the kernel parameter α affects, among other things, to the ripple of the spectral characteristic. Reduction of ripples was achieved by eliminating members of the Taylor series that predominantly influence on the ripple (Park & Schowengerdt, 1982). The analysis presented in (Meijering et al., 1999) indicates that $\alpha = -0.5$ is the optimal value of the kernel parameter for reducing the ripple of the spectral characteristic in the passband and stopband. Convolution interpolation realized by the parameterized cubic kernel is called PCC (Parametric Cubic Convolution) interpolation.

Increasing of the interpolation precision of the cubic interpolation kernel by constructing a two parameter (α, β) interpolation kernel (2P), was achieved (Hanssen & Bamler, 1999). The two parameter interpolation kernel is based on the

* Corresponding author: bojan.prlincevic@akademijakm.edu.rs

additional parameterization of the 1P Keys kernel. In the scientific literature, this kernel is called the 2P Keys kernel. Optimization of the 2P Keys kernel parameters in the estimation of the fundamental frequency, F_0, of the speech signal was determined in (Milivojević & Brodić, 2013) and (Milivojević et al., 2017). As a measure of the error estimate of the fundamental frequency MSE was used.

One parameter fifth-degree interpolation kernel, length L= 8, described in (Meijering et al., 1999). In order to increase of the precision of interpolation, the construction of a two parameter fifth-degree interpolation kernel was performed (Savić et al., 2021). The 2P fifth-degree interpolation kernel is constructed by the extended parameterization of the 1P fifth-degree interpolation kernel. The optimal parameters of the 2P fifth-degree interpolation kernel, when interpolating the audio signal, (α_{opt} = 0.1, β_{opt} = 0.0571), were determined using the experiment (Savić et al., 2022). The precision of the interpolation at 2P (MSE = $1.3253 \cdot 10^{-6}$) is higher than the precision of the interpolation at 1P kernel (MSE= $1.8096 \cdot 10^{-6}$).

In the previously cited papers, the analytical form of the spectral characteristic of the 2P fifth degre polynomial kernel, has not been determined. In this paper, the spectral characteristic of the 2P kernel, whose parameterization was done in (Savić et al., 2021), was calculated. The spectral characteristic of the 2P kernel is done as follows. It is first done by decomposing the 2P kernel into components. Then, by applying the Fourier transform to each kernel component, the spectral characteristics of each component were determined. In this way, the spectral components of the kernel are determined. Finally, taking into account all spectral components as well as the kernel parameters α and β, the spectral characteristic of the 2P kernel was determined. With the knowledge of the analytical form of the spectral characteristic, it is possible to change its shape by changing the kernel parameters, in order to bring its shape closer to the ideal box characteristic. In addition, the precision of interpolation in Digital Image, Audio and Speech processing can be affected by changing the kernel parameters, and thus minimize the interpolation error. This optimizes the kernel parameters. In this way, the scope of application of parametric convolutional kernels is increased.

Further organization of this paper is as follows. Section II describes: ideal kernel, 1P fifth order kernel, and 2P fifth order interpolation kernel. Section III describes the process of determining the spectral characteristic of the kernel. Section IV is the Conclusion

INTERPOLATION KERNELS

Ideal interpolation kernel

The ideal interpolation kernel for interpolating band limited signals is the form *sinc* = *sin*(x) / x (Keys, 1981). The definition of the *sinc* kernel is in the interval (-∞, +∞). Therefore, due to its infinite length, the *sinc* kernel cannot be realized. For this reason, it was necessary to truncated the *sinc* interpolation kernel to a finite length L (interval [-L / 2, L / 2]). The truncated *sinc* kernel, *sincw*, has a spectral characteristic that differs from the box characteristic. The difference is reflected in: a) the appearance of ripples of the spectral characteristics in the passband and stopband and b) finite slope of the spectral characteristics in the transition band (Savić et al., 2021). The ideal interpolation kernel *sinc* in the range (-20, 20) is shown in Fig. 1a. The spectral characteristics of the truncated kernel *sincw* for some lengths L (3, 5, 10, 20, + ∞) are shown in Figs. 1.b. The spectral characteristics of the ideal kernel *sinc* ($L \to \infty$) and the spectral characteristics in which the ripple increases with decreasing length L are indicated.

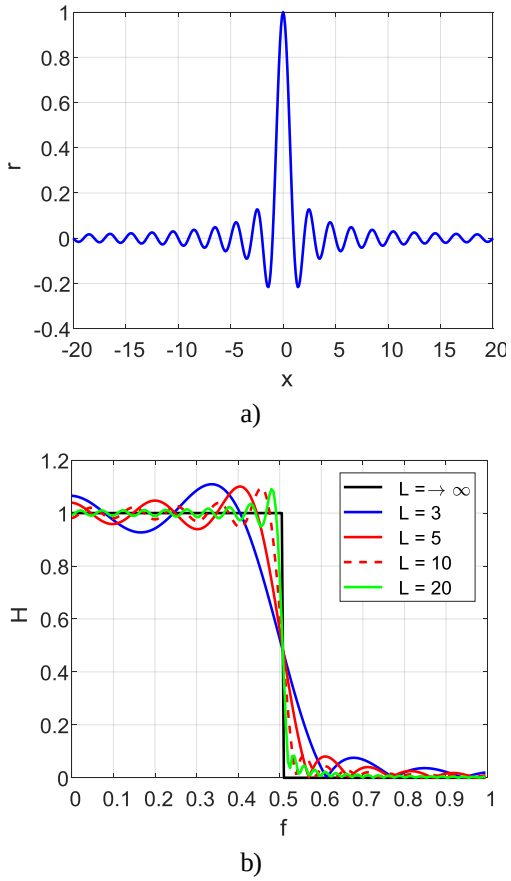

Figure 1. Interpolation kernel: a) time domain and b) spectral domain.

In order to reduce the numerical complexity, the *sinc* function is approximated by simpler mathematical functions. In the field of the Digital Signal Processing, DSP, and especially in the field of the Digital Image Processing, the approximation of the *sinc* function with polynomial functions is intensively used. In the field of Digital Image Processing, the interpolation kernels, formed from the third-order polynomials, are very popular. The most significant are the parameterized 1P, 2P and 3P Keys kernels (Hanssen & Bamler, 1999). The need to increase precision of the

interpolation has led to the construction of fifth-order polynomial interpolation kernels.

In the further part of this paper, the definition of one parameter and two parameter fifth-order kernels and their parameterization is described. After that, the spectral characteristic of the two parameter kernel was determined by applying the Fourier transform.

One parameter fifth-order kernel

The general form of the convolutional fifth-degree interpolation kernel is (Meijering et al., 1999):

$$r(x)=\begin{cases} a_5|x|^5+a_4|x|^4+a_3|x|^3+ & |x|\le 1\\ a_2|x|^2+a_1|x|+a_0, & \\ b_5|x|^5+b_4|x|^4+b_3|x|^3+ & 1<|x|\le 2\\ b_2|x|^2+b_1|x|+b_0, & \\ c_5|x|^5+c_4|x|^4+c_3|x|^3+ & 2<|x|\le 3\\ c_2|x|^2+c_1|x|+c_0, & \\ d_5|x|^5+d_4|x|^4+d_3|x|^3+ & 3<|x|\le 4\\ d_2|x|^2+d_1|x|+d_0, & \\ 0, & |x|>4 \end{cases}. \quad (1)$$

The coefficients of the kernel are determined subject to the following conditions: a) $r(0) = 1$, b) $r(x) = 0$ for $|x| = 1, \ldots, 4$; and c) $r^{(l)}(x)$ are continuous for $|x| = 0, \ldots, 4$. By parameterizing of the kernel, taking into account the previous conditions, form of the one parameter fifth-degree interpolation kernel is determined. The form of the 1P fifth-degree interpolation kernel is:

$$r(x)=\begin{cases} \left(10\alpha-\frac{21}{16}\right)|x|^5+\left(-18\alpha+\frac{45}{16}\right)|x|^4+ & |x|\le 1\\ \left(8\alpha-\frac{5}{2}\right)|x|^2+1, & \\ \left(11\alpha-\frac{5}{16}\right)|x|^5-\left(88\alpha-\frac{45}{16}\right)|x|^4+ & \\ (270\alpha-10)|x|^3-\left(392\alpha-\frac{35}{2}\right)|x|^2+ & 1<|x|\le 2\\ (265\alpha-15)|x|-(66\alpha-5), & \\ \alpha|x|^5-14\alpha|x|^4+78\alpha|x|^3- & \\ -216\alpha|x|^2+297\alpha|x|-162\alpha, & 2<|x|\le 3\\ 0 & |x|>3 \end{cases}, \quad (2)$$

where α is the kernel parameter.

Two parameter fifth-order kernel

In order to increase of the interpolation precision, a two parameter fifth-degree convolutional kernel is created. The process of kernel parameterization is presented in great detail in (Savić et al., 2021). The final form of the parametric 2P kernel is:

$$r(x)=\begin{cases} \left(10\alpha-10\beta-\frac{21}{16}\right)|x|^5+ & \\ \left(-18\alpha+18\beta+\frac{45}{16}\right)|x|^4+ & |x|\le 1\\ \left(8\alpha-8\beta-\frac{5}{2}\right)|x|^2+1, & \\ \left(11\alpha-11\beta-\frac{5}{16}\right)|x|^5+ & \\ \left(-88\alpha+88\beta+\frac{45}{16}\right)|x|^4+ & \\ (270\alpha-270\beta-10)|x|^3+ & 1<|x|\le 2\\ \left(-392\alpha+392\beta+\frac{35}{2}\right)|x|^2+ & \\ (265\alpha-265\beta-15)|x|+ & \\ (-66\alpha+66\beta+5), & \\ \alpha|x|^5+(-14\alpha+3\beta)|x|^4+ & \\ (78\alpha-30\beta)|x|^3+ & \\ (-216\alpha+112\beta)|x|^2+ & 2<|x|\le 3\\ (297\alpha-185\beta)|x|+ & \\ (-162\alpha+114\beta), & \\ \beta|x|^5-19\beta|x|^4+144\beta|x|^3- & \\ 544\beta|x|^2+1024\beta|x|-768\beta, & 3<|x|\le 4\\ 0, & |x|>4 \end{cases}, \quad (3)$$

where α and β are kernel parameters.

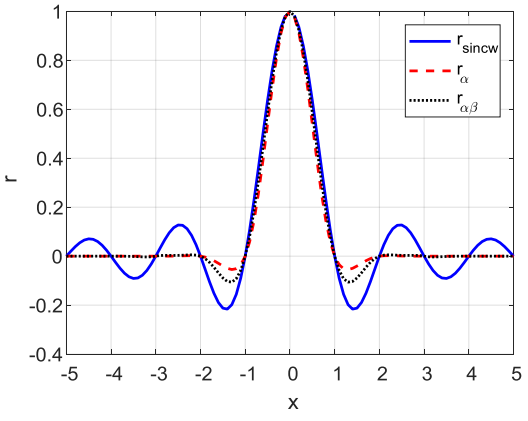

Figure 2. Truncated *sinc* ideally kernel, r_{sincw}, and fifth-order polynomial kernels: a) one parameter, r_α, and b) two parameter, $r_{\alpha\beta}$.

In fig. 2 are shown: a) truncated, i.e. windowizing ideally kernel, r_{sincw}, and b) 1P kernel, r_α, (Eq. (2)) and 2P kernel $r_{\alpha\beta}$ (Eq. (3)). Kernel parameters are $\alpha = 0.025$, $\beta = -0.04$. It can be

observed that the form of the two parameter, $r_{\alpha\beta}$, has a smaller deviation compared to the kernel r_{sincw}.

SPECTRAL CHARACTERISTICS OF THE 2P FIFTH-ORDER INTERPOLATION KERNEL

The algorithm for determining the spectral characteristic of the fifth-order kernel (Eq. (3)) was implemented in the following steps: a) decomposing the kernel into components, b) determining the spectral characteristics of each kernel component, and c) determining the spectral characteristics of the kernel depending on the parameters α and β.

2P kernel components

The 2P fifth-degree kernel (Eq. (3)) can be written in the form:

$$r(x) = r_0(x) + \alpha r_1(x) + \beta r_2(x), \tag{4}$$

where r_0, r_1 and r_2 are kernel components:

$$r_0(x) = \begin{cases} \frac{-21}{16}|x|^5 + \frac{45}{16}|x|^4 - \\ -\frac{5}{2}|x|^2 + 1 \\ \frac{-5}{16}|x|^5 + \frac{45}{16}|x|^4 - 10|x|^3 + \\ \frac{35}{2}|x|^2 - 15|x| + 5 \\ 0 \end{cases} \begin{array}{l} , \quad |x| \le 1 \\ \\ , \quad 1 < |x| \le 2, \\ \\ , \quad |x| > 2 \end{array} \tag{5}$$

$$r_1(x) = \begin{cases} 10|x|^5 - 18|x|^4 + 8|x|^2, & 0 < |x| \le 1 \\ 11|x|^5 - 88|x|^4 + 270|x|^3 - 392|x|^2 + & \\ +265|x| - 66, & 1 < |x| \le 2 \\ |x|^5 - 14|x|^4 + 78|x|^3 - 216|x|^2 + & \\ 297|x| - 162, & 2 < |x| \le 3 \\ 0; & |x| > 3 \end{cases}, \tag{6}$$

and

$$r_2(x) = \begin{cases} -10|x|^5 + 18|x|^4 - 8|x|^2 & 0 \le |x| \le 1 \\ -11|x|^5 + 88|x|^4 - 270|x|^3 + & 1 < |x| \le 2 \\ +392|x|^2 - 265|x| + 66 & \\ 3|x|^4 - 30|x|^3 + 112|x|^2 - & 2 < |x| \le 3 \\ -185|x| + 114 & \\ |x|^5 - 19|x|^4 + 144|x|^3 - & 3 < |x| \le 4 \\ -544|x|^2 + 1024|x| - 768 & \\ 0 & |x| > 4 \end{cases}. \tag{7}$$

As an example, the kernel components r_0, r_1 and r_2 are shown in Fig. 3.a. The ideal interpolation kernel, r_{sinc}, and the 2P fifth degree kernel, $r_{\alpha\beta}$, for α = 0.025 and β = -0.04 (Eq. (4)), on the interval [-5, 5], are shown in Fig. 3.b.

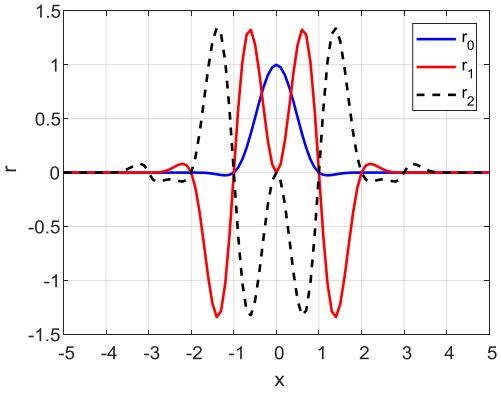

a)

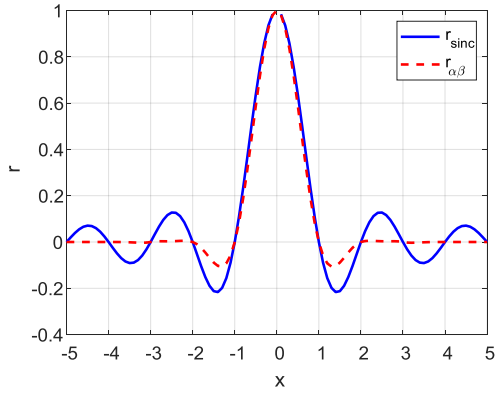

b)

Figure 3. Form of: a) kernel components r_0, r_1 and r_2, and b) ideal interpolation kernel, r_{sinc}, and the 2P fifth degree kernel, $r_{\alpha\beta}$, for α = 0.025 and β = -0.04.

Spectral characteristic of the kernel component

By applying of the Fourier transform over the 2P kernel r (Eq. 4), the spectral characteristic of the kernel is obtained:

$$\begin{aligned} H(f) &= FT\left(r_0(x) + \alpha r_1(x) + \beta r_2(x)\right) \\ &= H_0(f) + \alpha H_1(f) + \beta H_2(f) \end{aligned} \tag{8}$$

where H_0, H_1 and H_2 are the spectral components of the 2P kernel, respectively:

$$H_0(f) = \int_{-\infty}^{\infty} r_o(x) e^{-2\pi x f i} dx, \tag{9}$$

$$H_1(f) = \int_{-\infty}^{\infty} r_1(x) e^{-2\pi x f i} dx, \tag{10}$$

and

$$H_2(f) = \int_{-\infty}^{\infty} r_2(x) e^{-2\pi x f i} dx. \tag{11}$$

By replacing Eq. (5), (6) and (7) in (9), (10) and (11), respectively, the spectral components become:

$$
\begin{aligned}
H_0(f) = &\int_{-2}^{-1}\left(\begin{matrix}\frac{5}{16}x^5+\frac{45}{16}x^4+10x^3+\\ +\frac{35}{2}x^2+15x+5\end{matrix}\right)e^{-2\pi xfi}dx+\\
&\int_{-1}^{0}\left(\begin{matrix}\frac{21}{16}x^5+\frac{45}{16}x^4-\\ -\frac{5}{2}x^2+1\end{matrix}\right)e^{-2\pi xfi}dx+\\
&\int_{0}^{1}\left(\begin{matrix}\frac{-21}{16}x^5+\frac{45}{16}x^4-\\ -\frac{5}{2}x^2+1\end{matrix}\right)e^{-2\pi xfi}dx+\\
&\int_{1}^{2}\left(\begin{matrix}\frac{-5}{16}x^5+\frac{45}{16}x^4-10x^3+\\ +\frac{35}{2}x^2-15x+5\end{matrix}\right)e^{-2\pi xfi}dx
\end{aligned}, \quad (12)
$$

$$
\begin{aligned}
H_1(f) = &\int_{-3}^{-2}\left(\begin{matrix}-x^5-14x^4-78x^3-\\ -216x^2-297x-162\end{matrix}\right)e^{-2\pi xfi}dx+\\
&\int_{-2}^{-1}\left(\begin{matrix}-11x^5-88x^4-270x^3-\\ -392x^2-265x-66\end{matrix}\right)e^{-2\pi xfi}dx+\\
&\int_{-1}^{0}\left(-10x^5-18x^4+8x^2\right)e^{-2\pi xfi}dx+\\
&\int_{0}^{1}\left(10x^5-18x^4+8x^2\right)e^{-2\pi xfi}dx+\\
&\int_{1}^{2}\left(\begin{matrix}11x^5-88x^4+270x^3-\\ -392x^2+265x-66\end{matrix}\right)e^{-2\pi xfi}dx+\\
&\int_{2}^{3}\left(\begin{matrix}x^5-14x^4+78x^3-\\ -216x^2+297x-162\end{matrix}\right)e^{-2\pi xfi}dx
\end{aligned}, \quad (13)
$$

and

$$
\begin{aligned}
H_2(f) = &\int_{-4}^{-3}\left(\begin{matrix}-x^5-19x^4-144x^3-\\ -544x^2-1024x-768\end{matrix}\right)e^{-2\pi xfi}dx+\\
&\int_{-3}^{-2}\left(\begin{matrix}3x^4+30x^3+112x^2+\\ +185x+114\end{matrix}\right)e^{-2\pi xfi}dx+\\
&\int_{-2}^{-1}\left(\begin{matrix}11x^5+88x^4+270x^3+\\ +392x^2+265x+66\end{matrix}\right)e^{-2\pi xfi}dx+\\
&\int_{-1}^{0}\left(10x^5+18x^4-8x^2\right)e^{-2\pi xfi}dx+\\
&\int_{0}^{1}\left(-10x^5+18x^4-8x^2\right)e^{-2\pi xfi}dx+\\
&\int_{1}^{2}\left(\begin{matrix}-11x^5+88x^4-270x^3+\\ +392x^2-265x+66\end{matrix}\right)e^{-2\pi xfi}dx+\\
&\int_{2}^{3}\left(\begin{matrix}3x^4-30x^3+112x^2-\\ -185x+114\end{matrix}\right)e^{-2\pi xfi}dx+\\
&\int_{3}^{4}\left(\begin{matrix}x^5-19x^4+144x^3\\ -544x^2+1024x-768\end{matrix}\right)e^{-2\pi xfi}dx
\end{aligned}. \quad (14)
$$

Finally, the spectral components of the 2P kernel are

$$
H_0 = \frac{15\sin(f\pi)}{32f^6\pi^6}\left(\begin{matrix}-2f\pi\left(17\cos(f\pi)+\cos(3f\pi)\right)+\\ 21\sin(f\pi)+5\sin(3f\pi)\end{matrix}\right), \quad (15)
$$

$$
H_1 = \frac{3\sin(2f\pi)}{2f^6\pi^6}\left(\begin{matrix}66f\pi+50\sin(2f\pi)-5\sin(4f\pi)+\\ 2f\pi\left(26\cos(2f\pi)+\cos(4f\pi)\right)\end{matrix}\right), \quad (16)
$$

$$
H_2 = \frac{\sin(2f\pi)}{2f^6\pi^6}\left(\begin{matrix}-2f\pi\left(87+4f^2\pi^2+72\cos(2f\pi)\right)\\ -150\sin(2f\pi)+15\sin(4f\pi)-15\sin(6f\pi)\\ +2f\pi\left(\left(21-8f^2\pi^2\right)\cos(4f\pi)+3\cos(6f\pi)\right)\end{matrix}\right). \quad (17)
$$

In fig. 4 shows the spectral components of the 2P kernel, H_0, H_1 and H_2.

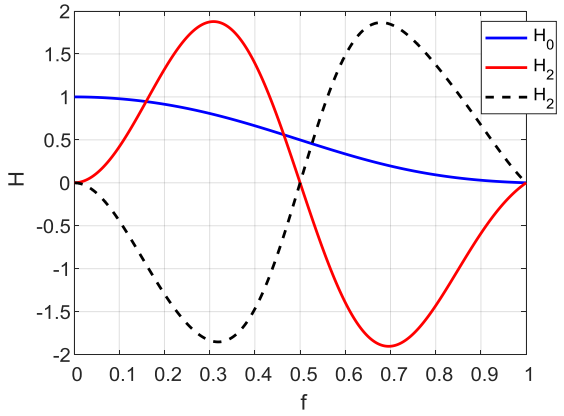

Figure 4. Spectral components of the 2P kernel, H_0, H_1 and H_2.

Spectral characteristics of the 2P kernel

The spectral characteristic of the 2P kernel, $H_{\alpha\beta}$, was obtained by substituting Eq. (15), (16) and (17) into (8). As an example, the spectral characteristics of:: a) ideal interpolation kernel, H_{sinc}, and b) 1P (H_α) and 2P ($H_{\alpha\beta}$) kernels, for α = 0.025 and β = -0.04, are shown in Fig. 5.

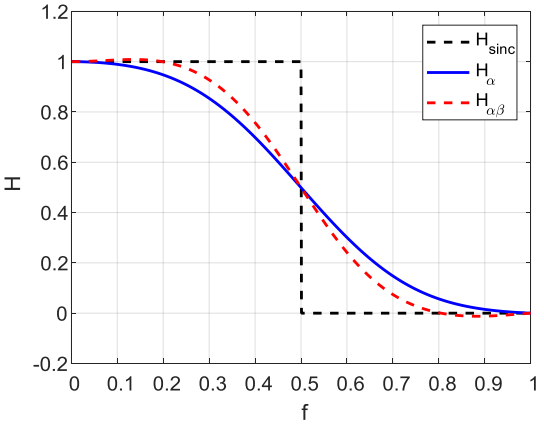

Figure 5. Spectral characteristics: a) ideal kernel, H_{sinc}, and b) 1P kernel, H_α, and 2P kernel, $H_{\alpha\beta}$, for kernel parameters α = 0.025 and β = -0.04.

It can be seen that the spectral characteristic of the 2P kernel, $H_{\alpha\beta}$, in relation to the spectral characteristic of the 1P kernel, H_{α}, has a better similarity with the box characteristic.

Further research will be based on optimizing the spectral characteristics of the 2P kernel in the spectral domain. The optimization will be aimed at minimizing the ripple of the spectral characteristic, and thus, towards greater similarity with the ideal box spectral characteristic.

CONCLUSION

In this paper, the spectral characteristic of two parametric fifth order polynomial interpolation kernels is calculated. By applying the Fourier transform, the spectral characteristic of the interpolation kernel was determined. Due to the finite length of the kernel, the spectral characteristic has ripples in the passband and stopband, as well as finite slopes in the transition band. Therefore, there is a deviation of the spectral characteristic of the 2P kernel from the characteristics of the ideal *sinc* interpolation kernel, that is, the box characteristic. By adjusting the kernel parameters α and β it is possible to minimize the ripple, and thus increase the similarity of the spectral characteristics of the kernel, with the box characteristic. Examples of minimizing the interpolation error, in Digital Image Processing, as well as in Audio and Speech Processing, are described in the scientific literature. In this way, the optimal values of the kernel parameters are determined. MSE is most often used as a measure of the interpolation precision.

Further research will be aimed at minimizing the ripples of spectral characteristic in the spectral domain. Minimization of the ripple will be carried out by analyzing the effect of the Taylor series members of the spectral characteristics that predominantly affect the ripple.

REFERENCES

Deng T. B. 2010. Frequency-domain weighted-least-squares design of signal-dependent quadratic interpolators, IET Signal Process., 4(1), pp. 102-111.

Dodgson N. 1997. Quadratic Interpolation for Image Resampling, IEEE Transactions On Image Processing, 6(9), pp. 1322-1326.

Hanssen R. & Bamler R. 1999. Evaluation of Interpolation Kernels for SAR Interferometry, IEEE Transactions on Geoscience and Remote Sensing, 37(1), pp. 318-321.

Keys, R. G. 1981. Cubic convolution interpolation for digital image processing' IEEE Trans. Acout. Speech, & Signal Processing, ASSP-29, pp. 1153-1160.

Meijering E. & Unser M. 2003. A Note on Cubic Convolution Interpolation, IEEE Transactions on Image Processing, 12(4), pp. 447-479.

Meijering E., Zuiderveld K. & Viegever M. 1999. Image Reconstruction by Convolution with Symmetrical Piecewise n^{th}-Order Polynomial Kernels', IEEE Transactions on Image Processing, 8(2), pp. 192-201.

Milivojević Z. & Brodić D. 2013. Estimation Of The Fundamental Frequency Of The Real Speech Signal Compressed By MP3 Algorithm, Archives of Acoustics, 38(3), pp. 363-373.

Milivojević Z., Savić N. & Brodić D. 2017. Three-Parametric Cubic Convolution Kernel For Estimating The Fundamental Frequency Of The Speech Signal, Computing and Informatics, 36, pp. 449-469.

Park K. S. & Schowengerdt R. A. 1982. Image reconstruction by parametric cubic convolution, Computer Vision, Graphics & Image Processing, 23, pp. 258-272.

Rifman S. S. 1973. Digital rectification of ERTS multispectral imagery, in Proc Symp. Significant Results Obtained From the Earth Resources Technology Satellite-1, 1(B) pp. 1131-1142.

Rukundo O. & Maharaj B. 2014. Optimization of image interpolation based on nearest neighbor algorithm, 2014 International Conference on Computer Vision Theory and Applications (VISAPP), 1, pp. 641-647.

Savić N. & Milivojević Z. 2022. Optimization of Parameters of the 2P Fifth Degree Interpolation Kernel for Interpolation of Audio Signals, 21st International Symposium INFOTEH-JAHORINA, pp. 207-210.

Savić N., Milivojević Z. & Prlinčević B. 2021. Development of the 2P Fifth-degree Interpolation Convolutional Kernel, International Journal of Innovative Research in Advanced Engineering (IJIRAE), 1(8), pp. 306-311.

Bulletin of Natural Sciences Research
Vol. 12, No. 1, 2022, pp. 21-27.

DOI: https://doi.org/10.5937/bnsr12-37850
Original Scientific Paper

ANALYSIS OF STATIC BEHAVIOR OF ION SENSITIVE FIELD EFFECT TRANSISTOR FOR PH MEASUREMENTS

TIJANA KEVKIĆ[1*], RESHMI MAITY[2], DRAGANA TODOROVIĆ[1], BILJANA VUČKOVIĆ[1], N. P. MAITY[2]

[1]Faculty of Sciences and Mathematics, University of Priština in Kosovska Mitrovica, Kosovska Mitrovica, Serbia
[2]Department of Electronics & Communication Engineering, Mizoram University (A Central University), Aizawl, India

ABSTRACT

The Ion-Sensitive Field-Effect Transistor (ISFET) is one of the most popular pH sensors traditionally using to measure hydrogen ion concentration (pH) of the electrolytic solutions. It is developed from Metal Oxide Semiconductor Field-Effect Transistor (MOSFET) by replacing gate electrode with an electrolytic solution to be tested, and a reference metal electrode immersed in that solution. Basic principle of ISFET operation is based on that of standard NMOS structure in conjunction with the insulator-electrolyte capacitor as described in this paper. The site-binding theory (generalized to two kinds of binding sites), together with the Gouy - Chapman-Stern model for the potential profile in the electrolyte, is coupled to the MOS physics. As a result, an approximate analytical model which completely describes static behavior of the ISFET is obtained. The developed description can serve as useful tool for understanding many contemporary biosensors based on original ISFET structure which has broad application in biomedicine, biological, chemistry and environmental areas.

Keywords: ISFET, pH sensor, MOSFET, Biosensors, Device simulation.

INTRODUCTION

In the last few decades, silicon based biosensors have found broad application in biomedical and environmental monitoring areas, high sensitive chemical detections, the diagnostic field, food industry etc. Main advantages of these biosensors over conventional ones are high sensitivity, rapid response, small size, the possibility of mass production and low cost (Bandiziol, 2015). Among a variety of types of silicon based biosensors, one of the most popular is the Ion-sensitive field-effect transistor (ISFET) based one. The ISFET was first introduced by Bergveld in the 1970 and it soon became the dominant device for measuring ion concentration (H^+ or OH^-) in the electrolytic solutions.

Generally, the ISFET is a type of potentiometric device that operates in a way similar to its purely electronic analogue, the MOSFET (Bergveld, 1981). Namely, the structures of these two transistors are identical except that metal gate in the ISFET is not immediate to the insulating layer. Instead, the gate is replaced by an electrolytic solution to be tested, with a reference metal electrode immersed in this solution. The reference electrode acts as a gate terminal allowing the ISFET to be biased in the same way as the standard MOSFET. When the ISFET is placed in an electrolyte, due to the interaction between the surface of the insulator and hydrogen ions in the electrolyte, a charge layer is created on the insulator surface and potential ψ_0 is generated at the electrolyte -insulator (EI) interface (Massobrio, 1991). Consequently, the threshold voltage and conductivity of the MOSFET channel are changed, and hence the current flowing through the channel. Therefore, to the ISFET could be applied same equations as for MOSFET with exception of the threshold voltage equation which had to be modified in order to include the effect of the EI interaction. In addition, pH sensitivity of the ISFET biosensor can be explained by examination of the effect of pH value of the electrolyte on the charge and potential distributions above the gate insulator (Si, 1979).

Over time, there have been outstanding advances in the modification of basic ISFET structure in accordance with various bio-sensing researching. For example, an enzymatically modified ISFET has been developed for the direct detection of penicillin (Caras, 1980), the enzyme-immobilized FET for detection of hydrogen ion concentration (Lee et al., 2009) and the DNA - modified FET based on deoxyribonucleic acid hybridization detection (Gasparyan, 2019), etc.

In this paper the ISFET is considered as a combination of the electrolyte - insulator capacitor and the standard NMOS transistor. For analyzing the potential changes at the EI interface a site-binding model was used. On the other side, the Gouy-Chapman-Stern model was used for description of the potential profile in the electrolyte. These two models are coupled to the MOSFET physics in order to explain the sensitivity of the ISFET device to hydrogen ion concentration in electrolytic solution. In this way, complete description of the ISFET static behavior is achieved.

* Corresponding author: tijana.kevkic@pr.ac.rs

OPERATING PRINCIPLE OF ISFET

The MOSFET is a basic building block of modern electronics. It has four terminals: source (S), gate (G), drain (D) and body (B). However, in many practical cases the body terminal is in connection with the source one thus forming a three-terminal device such as a field-effect transistor (Kevkić, 2018).

The abbreviation MOS refers to the three-layer transverse structure of the device. Namely, the substrate consists of a semiconductor, usually silicon p or n type. A thin insulating layer of silicon dioxide, briefly called gate insulator, is applied to the surface of the substrate. A metal gate electrode is placed above the insulator having the role of a control electrode. A positive voltage applied to the gate of MOSFET with p substrate generates a transverse electric field which leads to the repulsion of the holes present under the gate insulator. That results in creation of a depletion region which is populated by the bound negative charges. Simultaneously, the positive gate voltage pulls electrons from the substrate into the surface region under the gate insulator. When sufficient electrons are induced there, the substrate surface is inverted from p-type to n-type creating the thin inversion layer, i.e. the conduction channel. The gate voltage at which the channel forms is so-called the threshold voltage. Further, by applying voltage between the drain and source terminals V_{DS}, the current flows freely through the channel and its amount is controlled by the gate voltage (Kevkić, 2016; Kevkić 2018).

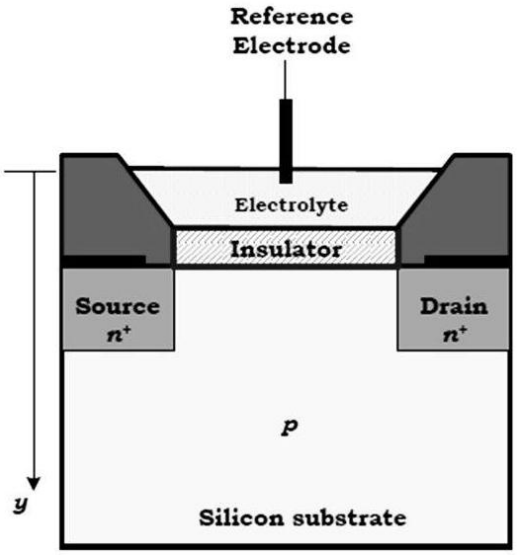

Fig. 1. Illustration of the ISFET structure.

The relative simple MOSFET structure has been served as a base for construction of the ISFET one which cross-section is schematically illustrated in Fig. 1. From figure is obvious that metal electrode in ISFET becomes a remote gate which is exposed to an electrolytic solution together to the gate insulator. The charge distribution at the EI interface is affects by any change of the hydrogen ion concentration of the solution. That change can be a consequence of the interaction of the gate insulator with the ions in the solution, as well as a horizontal electric field in the electrolyte when the voltage V_{DS} is applied (Tarasov, 2012).

In following will be described that basic mechanism of a pH-sensitive ISFET operation consists in the change of potential between the electrolytic solution and the gate insulator surface. As a consequence of that change the output current of ISFET I_d is increasing or decreasing. That is why, during the pH measurement, at a fixed input voltage at reference electrode of ISFET the change in I_d is observed. Therefore, the sensitivity of the ISFET device is relating to change in the output current, i.e. it can be expressed as I_d change per pH unit change (Heidari, 2018).

THE ISFET CONCEPT

During normal operation, the ISFETs as well as MOSFETs are usually biased in non-saturated mode. In this mode the threshold voltage V_T exhibits a linear relation with drain current (Dutta, 2012):

$$I_d = C_{ox}\mu\frac{W}{L}\left[\left(V_{GS}-V_T\right)V_{DS}-\frac{V_{DS}^2}{2}\right] \tag{1}$$

where C_{ox} is the gate insulator capacitance per unit area, μ is the effective surface mobility, W and L are the channel width and length, respectively, V_{GS} and V_{DS} are the gate-to-source and drain-to-source voltage, respectively.

The general threshold voltage of basic MOSFET is given by:

$$V_T = V_{FB} + 2\phi_F - \frac{Q_{dep}}{C_{ox}} \tag{2}$$

Here V_{FB} is flat-band voltage, Q_{dep} is the semiconductor surface depletion region charge density, ϕ_F is the Fermi potential of bulk silicon p-type given by $\phi_F = u_T \ln N_A/n_i$ where N_A is the doping acceptor concentration, n_i is the intrinsic carrier concentration in bulk, $u_T = kT/q$ is the thermal voltage. If we take into account relation for V_{FB}, the Eq. (2) can be rewritten in following form:

$$V_T = \phi_M - \phi_S + 2\phi_F - \left(\frac{Q_{ss}+Q_{ox}+Q_{dep}}{C_{ox}}\right) \tag{3}$$

Where ϕ_M and ϕ_S are the work function difference of the metal and semiconductor respectively, Q_{ss} is the surface state density at the substrate, Q_{ox} is fixed oxide charges.

For an ISFET fabricated on the same substrate and by using the same technology, since the electrolyte is in direct contact with the insulator, the flat band voltage changes due to the chemical changes that occur at the EI interface. Therefore, the expression for the threshold voltage of ISFET $V_T^{'}$ should include also terms which reflect the interfaces between the electrolyte and the gate insulator as well as the electrolyte and the reference electrode. Thus the threshold voltage of the ISFET is given by (Ytteralal, 2003):

$$V_T^{'} = \left(V_{ref} + \psi_{ij}\right) - \left(\psi_0 - \chi_{sol}\right) + V_T - \phi_M \tag{4}$$

where V_{ref} - the reference electrode potential with respect to vacuum and it is constant; ψ_{ij} - the potential difference between reference solution and electrolyte with typical value of 3 mV; χ_{sol} - surface dipole potential of the solution which is also constant and ψ_0 - potential of the electrolyte-insulator interface which is usually governed by the dissociation and association of the oxide surface groups (Bard, 1980).

According to Eq. (4), the threshold voltage of an ISFET is the sum of the threshold voltage of the MOSFET and the chemical part in which all terms are constant except ψ_0 which represents a chemical input parameter that depends on pH of electrolytic solution. It is clear that the main goal in ISFET applications is to represent the relation between ψ_0 and pH of the solution. In that purpose is utilizing the site- binding model considering silanol and amine groups as two possible kinds of binding sites (Bergveld, 2003).

Let us point out that for an ISFET, gate to source voltage V_{GS} is kept constant while the threshold voltage contains the variable input signal. On the other side, in the case of MOSFET, V_T is assumed to be constant and V_{GS} is the variable. However, in the basic electronic conception this difference will give no complications, because the so-called effective voltage defined as $V_{GS} - V_T$ can be seen in both cases as the actual input variable.

SITE – BINDING THEORY AND ELECTRICAL DOUBLE LAYER

Due to relative large radiuses and thermal motion, the ions of the dissolved species of the electrolyte cannot approach to the insulator surface (Yates, 1974). Opposite, hydrogen ions H^+ can approach to the surface of the insulator because they are small and not hydrated by water molecules. These ions can be accepted by amphoteric *Si –OH* sites that exist at the surface of the sensing SiO_2 insulator. As a result, the *Si –OH* sites became protonated, positively charged surface sites, i.e. $\left[Si - OH_2^+\right]$. On the other side, the surface amphoteric sites can also donate H^+ ions to the electrolyte becoming deprotonated, negatively charged ones $\left[Si - O^-\right]$. The exchange of H^+ ions between the electrolyte and the reactive surface sites can be described by following chemical reaction's equations (Bandizol, 2015):

$$\begin{aligned} &Si - OH \xleftarrow{K_a} Si - O^- + H_s^-; \\ &Si - OH + H_s^+ \xleftarrow{K_b} Si - OH_2^+ \end{aligned} \tag{5}$$

Here K_a and K_b are respectively the acidic and basic equilibrium constants of the surface reactions, given by:

$$K_a = \frac{\left[Si - O^-\right]\left[H_s^+\right]}{\left[Si - OH\right]}; K_b = \frac{\left[Si - OH_2^+\right]}{\left[Si - OH\right]\left[H_s^+\right]} \tag{6}$$

Where $\left[H_s^+\right]$ is the surface concentration of hydrogen ions. It is related to the bulk concentration $\left[H_B^+\right]$ through the Boltzmann relationship given by:

$$H_s^+ = H_B^+ \cdot \exp\left(-\frac{\psi_0}{u_T}\right) \tag{7}$$

Since the pH of the solution is $-\log H_B^+$, taking the minus logarithm of both sides of equation (7) results in key equation for formulating the relation between the ψ_0 to changes in the bulk pH:

$$pH_s = pH_B + \frac{\psi_0}{2.3 \cdot u_T} \tag{8}$$

According site – binding theory, the reactions of the ions present in the electrolyte and positively or negatively charged active sites present at the insulator surface result in the change of the total value of the active site charge at the insulator surface. This further means that insulator surface is charged with the surface charge density σ_0 which depends on the ion concentration in solution, i.e. on pH value of the solution. Due to charge neutrality, σ_0 is balanced by an equal but opposite charge σ_{dl} in the electrolyte. The charge σ_{dl} originated from ions which form the electrical double layer. According to the Gouy-Chapman-Stern model, the double layer which is formed at the vicinity of the EI interface consists of the Stern layer and the Gouy-Chapman diffuse layer (Tarasov, 2012; Lee, 2009). The Stern layer contains the adsorbed ions and is further divided into Inner Helmholtz Plane (IHP) and Outer Helmholtz Plane (OHP). The name of these planes originated from the Helmholtz condenser model used as a first approximation of the double layer which is very close to the interface. The IHP comprises of the counter ions specifically adsorb on the EI interface. The potential drop in IHP is

considerably sharp depending on the ions concentration present there. On the other side, the OHP is plane that passes through the centers of the hydrated non-specifically adsorbed ions at their distance of closest approach to the solid (Nakamura, 2011). The potential drop in OHP is less steep than in the IHP. Beyond the OHP the Gouy-Chapman diffuse layer extends into bulk of solution to the distance termed as Debye length, and represents the point to which the effect of the sensing surface is felt by the ions in the electrolyte.

It is clear that double layer may be considered as two parallel plate capacitors with equivalent capacitance given by:

$$C_e = \frac{C_{st} + C_{dl}}{C_{st} \cdot C_{dl}} \tag{9}$$

here C_{st} is constant capacitance called Stern capacitance and C_{dl} is the Gouy-Chapman diffuse layer capacitance. The value of C_{st} is 20 μF/cm^2, while C_{dl} is an order of magnitude greater than that. On the other side, the capacitance of the insulator layer C_{ox} is very low so the series of capacitances C_{st}, C_{dl} and C_{ox} results in a lower equivalent capacitance of the overall electrolyte-insulator-semiconductor (EIS) structure. As it is mentioned above, for electrolyte-insulator system holds the charge neutrality equation:

$$\sigma_0 = -\psi_0 C_e = -\sigma_{dl} \tag{10}$$

MODELING ELECTROLYTE – INSULATOR - SEMICONDUCTOR (EIS) STRUCTURE

Based onsite – binding theory and the Gouy-Chapman-Stern model, Bousse et al have modeled EIS system by introducing two parameters, pH_{pzc} and β (Hazarika, 2017). The parameter pH_{pzc} represents the point of zero charge that means the electrical neutral insulator surface. In this case the number of positive $\left[Si-OH_2^+\right]$ and negative $[Si-O^-]$ surface sites per unit area must be equal, and according to Eq. (6) and Eq. (7) we can get:

$$\left[H_S^+\right] = \left[H_B^+\right] = \sqrt{\frac{K_a}{K_b}} \tag{11}$$

Taking the minus logarithm of both sides of Eq. (11) we can obtain:

$$pH_{pzc} = -log\left(\sqrt{\frac{K_a}{K_b}}\right) \tag{12}$$

The second parameter β is the buffer capacity defined as the quantity of a strong acid or strong base that is added to one liter of the solution for changing it by one pH unit. For better understanding, buffer is a compound that resists change in pH when a limited amount of acid or base is added to it. Based on that, the β can be expressed as the ratio of the change in the number of the charged surface groups to the change in the pH_s:

$$\beta = \frac{d[B]}{dpH_S} \tag{13}$$

where $[B] = -\sigma_0 / q$.

The resulting equation for the potential drop ψ_0 between the electrolyte and the surface of the insulator, for relative large value of β is given by:

$$\psi_0 = 2.3u_T \frac{\beta}{\beta+1}\left(pH_{pzc} - pH\right) \tag{14}$$

In the case where the pH of the bulk solution is different from pH_{pzc} which usual value is 3, the insulator surface responses to that difference indicating how pH sensitive it is. Further, by using Eq. (10) for charge neutrality of EI system the effect of a small change in the surface pH on the change in the potential ψ_0 can be expressed as:

$$\frac{\partial\psi_0}{\partial pH_s} = \frac{\partial\psi_0}{\partial\sigma_0}\frac{\partial\sigma_0}{\partial pH_s} = -\frac{q\beta}{C_e} \tag{15}$$

By combining Eq. (15) with Eq. (7) the general expression for the pH sensitivity of insulator surface and, therefore ISFET device is obtained in following form:

$$\frac{\partial\psi_0}{\partial pH_B} = -2.3\frac{kT}{q}\cdot\alpha \tag{16}$$

with

$$\alpha = \left(2.3\frac{kTC_e}{q^2\beta}+1\right)^{-1} \tag{17}$$

The parameter α is a dimensionless sensitivity parameter of the ISFET gate insulator to pH of the bulk solution. Value of α varies between 0 and 1, depending on the β and the effective capacitance C_e. If α =1, the ISFET has a Nernstian sensitivity which is also the maximum achievable sensitivity (Lowe, 2015; Pijanowska, 2005).

ISFET STATIC MODEL

In Fig. 2 is shown the potential distribution in the EIS system along the y direction, normal to the interfaces. Here, by ψ_d, ψ_0 and ψ_s are denote the electric potentials at the edge of diffuse layer (OHP), at the electrolyte - insulator interface, and at the semiconductor - insulator interface, respectively.

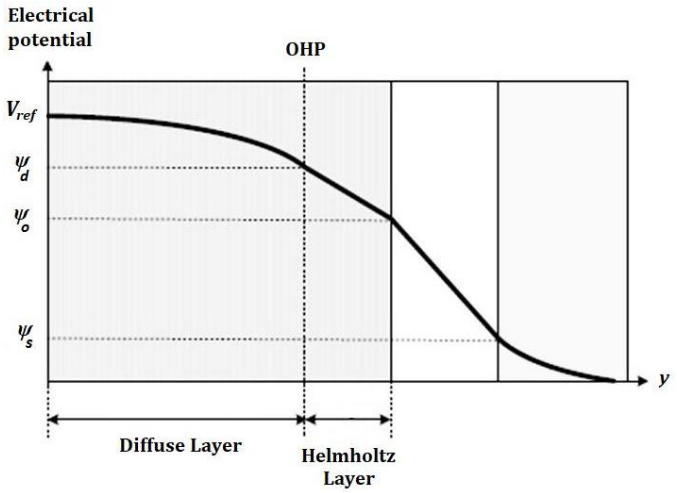

Fig. 2. Potential distribution in an EIS system along the direction normal to the interface.

Equation of the charge neutrality of the EIS system can be expressed by following sum:

$$\sigma_0 + \sigma_{dl} + Q_s = 0 \tag{18}$$

where σ_0 and σ_{dl} are the charge on the electrolyte - insulator interface and through the diffuse layer, respectively, while Q_s is the charge density in the semiconductor and is given by:

$$Q_s = \pm\sqrt{(2\varepsilon_s kTp_0)}\times \left[\frac{\psi_s}{u_T} - 1 + exp(-\frac{\psi_s}{u_T}) + \frac{n_0}{p_0}(-\frac{\psi_s}{u_T} - 1 + exp\left(\frac{\psi_s}{u_T}\right)\right]^{\frac{1}{2}} \tag{19}$$

Here ε_s is dielectric permittivity of semiconductor; p_0 and n_0 are the equilibrium concentrations of holes and electrons, respectively. Sign „plus" is taken for $\psi_s \prec 0$ and "minus" for $\psi_s \succ 0$.

Otherwise the charge density Q_s is related to ψ_0 and ψ_s through Gauss law (Passeri, 2015):

$$Q_s = C_{ox}\left(\psi_s - \psi_0\right) \tag{20}$$

On the other hand, using a Gaussian surface which encompasses the charge σ_{dl} and passing through the Stern layer it holds (Wu, 2015):

$$\sigma_{dl} = C_{st}\left(\psi_s - \psi_0\right) \tag{21}$$

Further, if the Stern layer and the diffuse layer are considered as two capacitors in series, the potential drop ψ_0 between the solution and the insulator surface can be expressed as:

$$\psi_0 = \frac{\sigma_0 C_{st} C_{dl}}{C_{st} + C_{dl}} \tag{22}$$

where C_{dl} is the diffuse layer unit-area capacitance given by:

$$C_{dl} = \left(\frac{q^2 c_0 \varepsilon_w \varepsilon_0}{kT}\right)^{1/2} \tag{23}$$

here ε_w is dielectric constant of water and c_0 is the solution concentration.

Also, relationship between charge σ_{dl} and potential ψ_d can be obtained by solving the Poisson equation in the diffuse layer, i.e.

$$\sigma_{dl} = -\sqrt{8kT\varepsilon_w\varepsilon_0 c_0}\,sinh\left(\frac{V_{ref} - \psi_d}{2u_T}\right) \tag{24}$$

Second, by considering two kinds of the binding sites on the insulator surface the surface charge density is given by:

$$\sigma_0 = qN_s\left[\left(\frac{[H_S^+]^2 - K_a K_b}{[H_S^+]^2 + K_a\left[H_S^+\right] + K_a K_b}\right)N_{sil} + \left(\frac{[H_S^+]}{\left[H_S^+\right] + K_N^+}\right)N_{nit}\right] \tag{25}$$

Where N_s is the total number of available surface binding sites per unit area, while N_{sil} and N_{nit} are that of silanol and primary amine sites and K_N^+ is dissociation constants for positively charged amine sites.

Combining the above equations give the potential ψ_0 as function of hydrogen ion concentration in the solution (Jiao, 2012):

$$\psi_0(H_s) = \frac{qN_s}{C_{dl}}\left(\frac{[H_S^+]^2 - K_a K_b}{[H_S^+]^2 + K_a\left[H_S^+\right] + K_a K_b}\right) + 2u_T sinh^{-1}\left[qN_s S\left(\frac{[H_S^+]^2 - K_a K_b}{[H_S^+]^2 + K_a\left[H_S^+\right] + K_a K_b}\right)\right]\frac{1}{\sqrt{8kTc_0\varepsilon_w}} \tag{26}$$

This equation together with equation (7) show that the change in the pH of electrolyte leads to the change in the surface potential ψ_0 which in turn leads to the change in the threshold voltage. In this way is obtained a set of equation that presents the base of the ISFET static model with two kinds of binding sites.

RESULTS AND DISSCUSION

In this paper is consider an ISFET pH sensor with channel length $L = 1.3 \cdot 10^{-6} m$; channel width $W = 10^{-6} m$ and effective insulator thickness $t_{ins} = 4 \cdot 10^{-8} m$. The concentration of acceptor atoms in region of channel is $N_A = 2 \cdot 10^{-18} cm^{-3}$. The other parameter values used for simulation are shown in Table 1.

Table 1. The parameter value used for simulation.

K_a	$15.8 mol/l$
K_b	$63.1 \cdot 10^{-9}\ mol/l$
C_{st}	$2 \cdot 10^{-5}\ F/cm^2$
$n_0(inv) \approx p_0$	$2 \cdot 10^{15}\ cm^{-3}$
T	$300 K$
n_i	$1.43 \cdot 10^{10}\ cm^{-3}$
ε_w	50
c_0	$0.015 mol/l$
χ_{soi}	$3 \cdot 10^{-3} V$
d_{OHP}	$3 \cdot 10^{-10}\ m$
u_T	$26\ mV$

Set of above equations was implemented in software package MATHEMATICA 11.0 to simulate the static behavior of ISFETs. Fig. 3. shows the drain current of SiO_2-gate ISFET when the reference electrode was exposed to different pH electrolytes. The reference voltage and the drain voltage were kept at 2 V and 0.8 V, respectively.

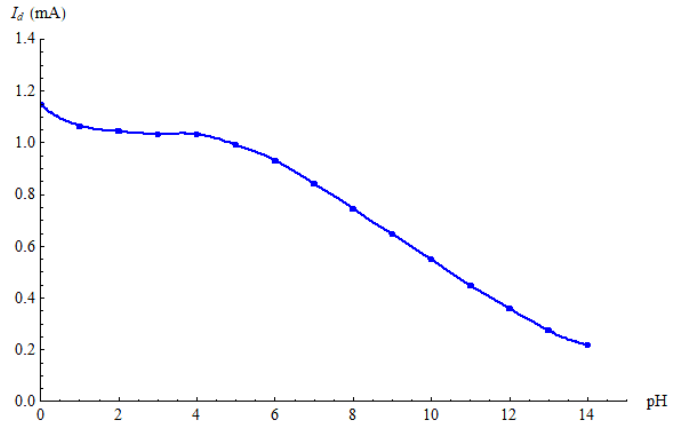

Fig. 3. The drain current of ISFET as a function of pH at $V_{ref} = 2V$ and $V_{DS} = 0.8V$.

From Fig. 3. is clear that the drain current is almost constant for pH value from 2 to 4. It means that I_d is less sensitive to that pH region, which is corresponding to the point of zero charge pH_{pzc} at which the insulator surface is neutral, i.e. there is no net charge $(\sigma_0 = 0)$.

The drain current of considered ISFET device as a function of the applied gate (reference) voltage is presented in Fig. 4. The $I_d(V_{GS})$ curve in Fig. 4. has similar shape as at a regular MOSFET. In the other words, this curve shows that the ISFET is working same as a regular MOSFET but the threshold voltage is increased in the ISFET case what is expected in accordance with Eq. (4).

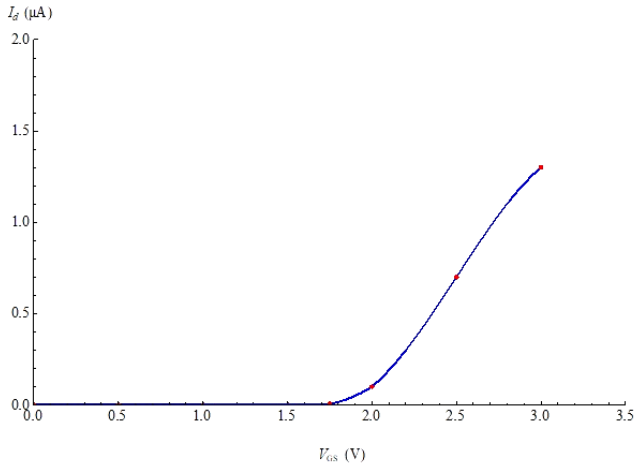

Fig. 4. The drain current of ISFET as a function of the reference electrode voltage V_{GS}.

Fig. 5. shows the output $I_d(V_{DS})$ characteristics of considered ISFET device for three different pH values of the electrolytic solution. The reference voltage V_{GS} was kept to 2.6 V. It is obvious that the drain current of ISFET device decreases such as the pH value of tested electrolyte increases.

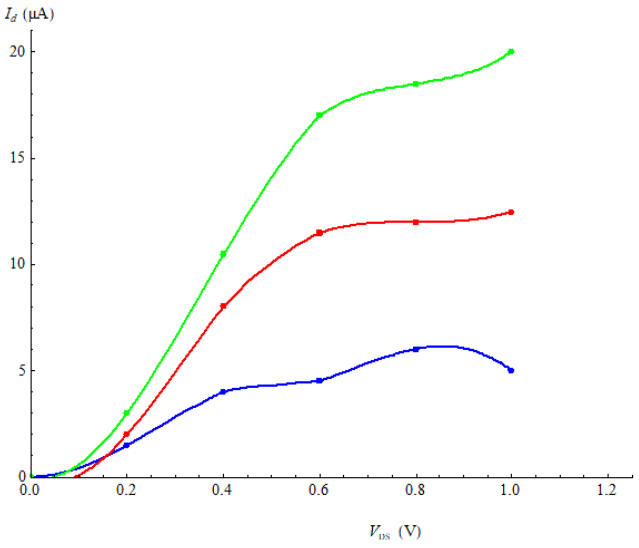

Fig.5. Drain current as a function of the drain to source voltage for pH value of 3 (green line), 7 (red line) and 11 (blue line).

CONCLUSION

In this work, the static behavior of ISFET which is using as a pH sensor is studied. The considered device includes a SiO_2-gate ISFET biased by the AgCl reference electrode, an n-channel MOSFET whose gate is controlled by a controllable external voltage. Statistical behavior of analyzing device is described by the approximate analytical model based on charge and potential equations of an electrolyte – insulator - semiconductor structure. By solving these equations in regions of semiconductor channel, the insulator - electrolyte interface and the diffuse layer respectively, the drain current related of each pH is obtained. The results obtained by implementation of the derived sets of equations in MATHEMATICA 11.0. confirm the prediction of sensitivity study that the drain current is less sensitive to pH of the electrolyte near the point of zero charge, $2<pH<4$, in the case of SiO_2-gate ISFETs.

The described model can be applied to the ISFET with gate insulator and reference electrode made of the materials that differ from considered, standard case. Moreover, it can be broad to the ISFET device with appropriate selective membranes what the subject of some future paper. Further, the structure of the fundamental set of equations could be easily modified in order to describe, at the physical level, more complex phenomena.

ACKNOWLEDGMENTS

Authors thank the Ministry of Education, Science and Technological Development of the Republic of Serbia for support under Contract No. **451-03-68/2022-14** and the Faculty of Sciences and Mathematics in Kosovska Mitrovica (University of Priština in Kosovska Mitrovica, Department of Physics) for support under the project **ИЈ-0201**.

REFERENCES

Bandiziol, A., Palestri, P., Pittino, F., Esseni, D. & Selmi, L. 2015. A TCAD-Based Methodology to Model the Site-Binding Charge at ISFET/Electrolyte Interfaces. IEEE Transactions on Electron Devices, 62(10), pp. 3379- 3386.

Bard, A. J., Faulkner, L. R., Leddy, J. & Loski, C. G. 1980. Electrochemical methods: fundamentals and applications, Wiley New York.

Bergveld, P. 1981. The operation of an ISFET as an electronic device, Sensors and Actuators, 1, pp. 17-29.

Bergveld, P. 2003. ISFET, theory and practice. IEEE Sensor Conference, Toronto 2003.

Caras, S. & Janata, J. 1980, Field effect transistor sensitive to penicillin, Anal. Chem., 52, pp. 1935–1937.

Dutta, J. C. 2012. Ion-Sensitive Field-Effect Transistor for applications in bioelectronics sensors: A research review. IEEE 2nd National Conference of Comptational Intelligence and Signal Processing (CISP), pp. 185-191. Cross ref

Gasparyan, L., Mazo, I., Simanyan, V. & Gasparyan, F. 2019. ISFET based DNA sensor: Current-voltage characteristics and sensitivity to DNA molecules. Open Journal of Biophysics, pp. 239-253.

Hazarika, Ch. & Sharma S. 2017. Survey on Ion-Sensitive Field-Effect Transistor from the view point of ph sensitivity and drift. Indian Journal of Science and Technology, 10(37), pp. 1-18.

Heidari, S. & Karami, M. A. 2018. Ion-sensitive field-effect transistor performance enhancement with high bandgap semiconductor, 17th International Meeting on Chemical Sensors – IMCS, pp. 645-646.

Jiao, L. & Barakat, N. 2012. Ion-sensitive field-effect transistor as a pH sensor. Journal of Nanoscience and Nanotechnology, 12, pp. 1-5.

Kevkić, T. & Stojanović, V. 2018. Interpolation Logistic Function in the Surface Potential Based MOSFET Modeling. Univ. thought, Publ. nat. sci., 8(2), pp. 73-78. Doi: 10.5937/univtho8-17067.

Kevkić, T., Stojanović, V. & Petković, D. 2016. Modification of the transition's factor in the surface potential based MOSFET model. Univ. thought, Publ. nat. sci., 6(2) pp. 55-60. doi:10.5937/univtho6-1360

Lee, C. S., Kim, S. K. & Kim M. 2009. Ion-sensitive field-effect transistor for biological sensing. Sensors, 9, pp. 7111-7131. doi:10.3390/s90907111

Lowe, B. M. L., Sun, K., Zeimpecis, I., Skylaris, C, K. & Green G. N. 2017. Field-effect sensors-from pH sensing to biosensing: sensitivity enhancement using streptavidin-biotin as a model system. The Analyst 142(22), pp. 4173-4200. https://doi.org/10.1039/C7AN00455A

Nakamura, M., Sato, N., Hoshi, N. & Sakata, O. 2011. Outer Helmholtz Plane of the Electrical Double Layer Formed at the Solid Electrode-Liquid Interface. Chem-PhysChem, 12, pp. 1430-1434. https://doi.org/10.1002/cphc.201100011

Passeri D., Morozzi A., Kanxheri K., Scorzoni A., 2015. Numerical simulation of ISFET structures for biosensing devices with TCAD, BioMed Eng OnLine, pp. 425-435.

Pijanowska, D. & Torbicz, W. 2005. Biosensors for bioanalytical applications. Bull. Pol. Acad. Sci. - Tech. Sci, 53, pp. 251-260.

Tarasov, A., Wipf, M., Stoop, R. L., Bedner, K., Fu, W., Guzenko, V. A., Knopfmacher, O., Calame, M. & Scho, C. 2012. Understanding the electrolyte background for biochemical sensing with ion-sensitive field-effect transistors. ACS Nano, 6, pp. 9291-9298.

Si, W. M. & Cobbold, R. S. C. 1979. Basic properties of the electrolyte – SiO_2 –Si system: Physical and theoretical aspects, IEEE Transactions on Electron Devices, 26, pp. 1805-1815.

Wu, X. & Jia, A. Z., 2015. Analysis and simulation on an isfet with back-gated structure and high-mobility channel material. Int. Conference CISIA 2015, pp. 883-885.

Yates, D. E., Levine, S. & Healy, T. W. 1974. Site-binding model of the electrical double layer at the oxide/water interface. Journal of the Chemical Society, Faraday Transactions 1: Physical Chemistry in Condensed Phases, 70, pp. 1807-1818.

Ytteralal, T., Cheng, Y. & Fjeldly, T. A., 2003. Device Modeling for Analog and RF CMOS Circuit Design. John Wiley & Sons, New York.

CIP - Каталогизација у публикацији
Народна библиотека Србије, Београд

5

BULLETIN of Natural Sciences Research / editor in chief Stefan R. Panić. - [Štampano izd.]. - Vol. 10, no. 2 (2020)- . - Kosovska Mitrovica : Faculty of Sciences and Mathematics, University of Priština, 2020- (Kruševac : Sigraf). - 29 cm

Polugodišnje. - Je nastavak: The University thought. Publication in natural sciences = ISSN 1450-7226. – Drugo izdanje na drugom medijumu: Bulletin of Natural Sciences Research (Online) = ISSN 2738-1013
ISSN 2738-0971 = Bulletin of Natural Sciences Research (Štampano izd.)
COBISS.SR-ID 28586505

Available Online

This journal is available online. Please visit http://www.bulletinnsr.com to search and download published articles.